

phytools 2.0: An updated R ecosystem for phylogenetic comparative methods (and other things)

Liam J. Revell^{1, 2}

¹Department of Biology, University of Massachusetts Boston, Boston, MA, USA

²Facultad de Ciencias, Universidad Católica de la Santísima Concepción, Concepción, Chile

Corresponding author:

Liam J. Revell^{1,2}

Email address: liam.revell@umb.edu

ABSTRACT

Phylogenetic comparative methods comprise the general endeavor of using an estimated phylogenetic tree (or set of trees) to make secondary inferences: about trait evolution, diversification dynamics, biogeography, community ecology, and a wide range of other phenomena or processes. Over the past ten years or so, the *phytools* R package (Revell 2012) has grown to become an important research tools for phylogenetic comparative analysis. *phytools* is a diverse contributed R library now consisting of hundreds of different functions covering a variety of methods and purposes in phylogenetic biology. As of the time of writing, *phytools* included functionality for fitting models of trait evolution, for reconstructing ancestral states, for studying diversification on trees, and for visualizing phylogenies, comparative data, and fitted models, as well numerous other tasks related to phylogenetic biology. Here, I describe some significant features of and recent updates to *phytools*, while also illustrating several popular workflows of the *phytools* computational software.

1 INTRODUCTION

Phylogenetic trees are the directed graphs used to represent historical relationships among a set of operational taxa that are thought to have arisen via a process of descent with modification and branching (Felsenstein 2004; Harmon 2019). Operational taxa in a reconstructed phylogenetic tree might be gene copies, paralogous and orthologous members of a gene family, viral sequences, whole genomes, human cultural groups, or biological species (Nunn 2011; Yang 2014). According to its broadest definition, the phylogenetic comparative method corresponds to the general activity of using a known or (most often) estimated phylogenetic tree to learn something *else* (apart from the relationships indicated by the tree) about the evolutionary process or past, the contemporary ecology, the biogeographic history, or the origins via diversification, of the particular taxa of our phylogeny (Harvey and Pagel 1991; Felsenstein 2004; Nunn 2011; OMeara 2012; Harmon 2019; Revell and Harmon 2022).

Phylogenetic comparative methods are not new. Perhaps the most important article in the development of the phylogenetic approach to comparative biology (Felsenstein 1985) was first authored nearly 40 years ago, and was even the subject of a recent retrospective (Huey et al. 2019). Nonetheless, it's fair to say that phylogenetic comparative methods have seen a relatively impressive expansion and diversification over the past two decades (e.g., Butler and King 2004; Felsenstein 2005; O'Meara et al. 2006; Maddison et al. 2007; Hohenlohe and Arnold 2008; Revell and Collar 2009; Morlon et al. 2010; Stadler 2011; Etienne and Haegeman 2012; Goldberg and Igić 2012; Beaulieu et al. 2013; Rabosky 2014; Uyeda and Harmon 2014; Beaulieu and O'Meara 2016; Revell 2021; MacPherson et al. 2022, and many others; reviewed in OMeara 2012; Garamszegi 2014; Harmon 2019; Revell and Harmon 2022). This has included the development of new approaches for studying the generating processes of trees (that is, speciation and extinction), the relationship between phenotypic traits and species diversification, and a range of techniques for investigating heterogeneity in the evolutionary process across the branches and clades of

the tree of life (OMeara 2012; Harmon 2019; Revell and Harmon 2022).

Phylogenetic comparative methods have also begun to be applied extensively outside of their traditional domain of evolutionary research. In particular, phylogenies and the comparative method have made recent appearances in studies on infectious disease epidemiology, virology, cancer biology, sociolinguistics, biological anthropology, molecular genomics, and community ecology, among other disciplines (e.g., Moura et al. 2016; Baele et al. 2018; Bentz et al. 2018; Beale et al. 2019; Bushman et al. 2019; Sánchez-Busó et al. 2019; Valles-Colomer et al. 2019; Freitas et al. 2020; Jezovit et al. 2020; Blinkhorn and Grove 2021; McLaughlin et al. 2022; Pepke and Eisenberg 2022; Pozzi et al. 2022; Compton et al. 2023; Mifsud et al. 2023; Van Borm et al. 2023, and many others).

The scientific computing environment R (R Core Team 2023) is widely-used in biological research. One of the major advantages that R provides is that it empowers computational scientists and independent developers to build functionality on top of the basic R platform. This functionality often takes the form of what are called contributed R packages: libraries of related functions built by individuals or research collaboratives not part of the core R development team. The growth of importance of R in phylogenetic biology stems entirely from contributed R package. Among these, the most important core function libraries are *ape* (Paradis et al. 2004; Popescu et al. 2012; Paradis and Schliep 2019), *geiger* (Harmon et al. 2008; Pennell et al. 2014), *phangorn* (Schliep 2011), and my package, *phytools* (Revell 2012).

phytools is an R function library dedicated primarily to phylogenetic comparative analysis, but also including approaches and methodologies in a range of other domains of phylogenetic biology – not restricted to, but especially, visualization. The original article describing *phytools* is now more than ten years old, and though I recently published a more comprehensive book on the subject of phylogenetic comparative methods in the R environment (Revell and Harmon 2022), I nonetheless felt that it was time to provide a briefer (although this article is by no means brief) update of *phytools* specifically – for the primary scientific literature. This is the main purpose of the current article.

The *phytools* library has now grown to be very large – consisting of hundreds of functions, a documentation manual that's more than 200 pages in length, and tens of thousands of lines of computer code. As such, I thought it would be most useful to compactly summarize some of the functionality of the *phytools* R package in a few different areas, but each time provide a small set of more detailed example analytical workflows (computational “vignettes”) for the current 2.0 version of the *phytools* package.

2 OVERVIEW

The *phytools* R package contains functionality in a diversity of different research areas of phylogenetics and phylogenetic biology. Rather than attempt a comprehensive survey of this functionality here, what I've elected to do instead is briefly review a smaller number of methodological areas, and then illustrate each of these with multiple analysis workflows – including the corresponding R code that can be used to reproduce the analysis and results presented.

My hope is that this article will serve as more than the typical software note placeholder for *phytools*, and may instead aid R phylogenetic users, both new and old, to be inspired to apply some of the methodologies illustrated herein to their own questions and data. On the other hand, even though it takes the form of a tutorial or R package vignette, this article is not intended to cover nor fully enumerate the complete range of functionality of the package. For that, I would refer readers to the *phytools* software documentation, my recent book with Luke Harmon (Revell and Harmon 2022), and my *phytools* development blog (<http://blog.phytools.org>).

3 INSTALLING AND LOADING PHYTOOLS

This article assumes that readers already have some familiarity with the R computing environment, and have previously installed contributed R packages. Nonetheless, to get started using *phytools*, the easiest way to install the package locally is by using the R base function called `install.packages` (in our case, `install.packages("phytools")`), which will download and install *phytools* from its CRAN page. (CRAN is an acronym for Comprehensive R Archive Network: a network of mirror repositories used both to archive and distribute R and contributed R packages.) Readers undertaking phylogenetic analysis in the R environment for the first time will note that when we ask R to install *phytools*, several other R packages are also downloaded and installed automatically. These are packages upon which *phytools* depends – meaning that *phytools* uses one or multiple functions exported by each

of these packages in its own internal R code. More will be said later about the dependency relationship between *phytools* and other packages of the R and R phylogenetic ecosystems.

Having installed *phytools*, if we'd like to proceed and use it in an interactive R session, we'd normally load it. Loading an R package simply makes the names of the functions of that package visible and available in our current R session. This can be done using the base R function `library`.

```
library(phytools)
packageVersion("phytools")
```

```
## [1] '1.9.18'
```

`packageVersion` tells us which version of *phytools* we have installed. Readers hoping to follow along should ensure that they have a *phytools* package version that matches or exceeds the value they see above. The *phytools* package is now loaded.

4 DISCRETE CHARACTERS

The *phytools* R library now contains a wide range of different methods and models for the analysis of *discrete character evolution* on trees. For example, *phytools* can be used to fit and plot an extended *Mk* model, the continuous-time Markov chain model usually employed to study discrete character evolution on trees (*phytools* function `fitMk`, Lewis 2001; Harmon 2019), it can fit Pagel's correlational binary trait evolution model (`fitPagel`, Pagel 1994), it can be used to perform stochastic character mapping and reconstruct ancestral states under the *Mk* and threshold models (`make.simmap`, `simmap`, `ancThresh`, and `ancr`, Huelsenbeck et al. 2003; Felsenstein 2005, 2012; Revell 2014a), it can fit a polymorphic trait evolution model (`fitpolyMk`, Revell and Harmon 2022), it can fit a hidden-rates model (`fitHRM`, Beaulieu et al. 2013), it can compare the rate of discrete character evolution between clades and trees (`fitmultiMk` and `ratebytree`, Revell et al. 2018; Revell and Harmon 2022), and it can simulate discrete character data under multiple models (e.g., `sim.Mk`, `sim.history`, `sim.multiMk`).

In this section, I'll illustrate the use of just a few of the different discrete character methods that have been implemented in the *phytools* software.

4.1 Stochastic character mapping

Perhaps the most important and widely-used discrete character analysis of *phytools* is a popular technique referred to as "stochastic character mapping" (Nielsen 2002; Huelsenbeck et al. 2003; Bollback 2006). Stochastic character mapping is a method in which we randomly sample discrete character histories ("stochastic maps") of our trait on the tree under a specified model. By sampling these character histories from their probability distribution under our trait evolution model, and then integrating over the set of histories that we obtain, stochastic mapping helps us to develop a more complete picture of the evolutionary history of our character trait of interest: in terms of the number and types of evolutionary change the character may have undergone; the marginal probabilities that each node of the tree may have been in each condition of the trait; and the branches of the tree with more or fewer character state changes.

Stochastic mapping in *phytools* can be undertaken in more than one way. An example of a stochastic character mapping analysis could be to first fit (e.g., using Maximum Likelihood) the character transition model (a variant of the *Mk* discrete character evolution model of Lewis 2001; also see, OMeara 2012; Harmon 2019; Revell and Harmon 2022), and then proceed to randomly sample a set of perhaps 100 or 1,000 stochastic character histories – each consistent with the phenotypic trait observations that we have for the terminal taxa of our tree, and obtained in proportion to their probability under our fitted model. (Other workflows are also popular and possible to undertake within R. For instance, rather than use a single, fixed model of character evolution that's been optimized using Maximum Likelihood, one might instead sample parameters of the evolutionary process from their joint posterior probability distribution using Bayesian MCMC. See Revell and Harmon 2022 for more details.)

To illustrate stochastic mapping here, I'll use a discretely-valued, ecological trait for a small phylogeny of centrarchid fishes from Revell and Collar (2009). Since the trait (which we'll refer to as "feeding mode") is binary, meaning that it only takes two levels, there are a total of four possible discrete character (extended *Mk*, see Harmon 2019) models: equal back-and-forth transitions between the two character values; different rates; and then the two different irreversible trait evolution models.

146 *phytools* now allows us to fit a single model or any arbitrary set of models, compare them (if applicable),
 147 and pass the model weights and fitted models directly to our stochastic mapping function. If the input
 148 is a set of models, as it will be in our example below, our function (called `simmmap`) will then proceed
 149 to automatically sample stochastic character histories with probabilities that are proportional to each
 150 model weight. Experienced *phytools* users may figure out that `simmmap` is just a sophisticated wrapper
 151 function of `make.simmmap` – the traditional method used for undertaking stochastic character mapping
 152 in *phytools*. A major advantage of sampling stochastic maps across a set of models, rather than under our
 153 single best model, is that it allows us to integrate over model uncertainty in direct proportion to the weight
 154 of evidence favoring each model in our set.

155 For this example, and all subsequent examples of the article, our data have been packaged with the
 156 *phytools* library – so we can easily load them in an interactive R session using the base R `data` function,
 157 as follows.

```
data(sunfish.tree)
data(sunfish.data)
```

158 For our *Mk* model-fitter (which here will be the *phytools* function `fitMk`), and for the other discrete
 159 character methods of the *phytools* R package, our input phenotypic trait data typically take the form of
 160 a character or factor vector. Personally, I prefer to use factors, because in that case we can more easily
 161 access the levels assumed by the character through a call of the base R function `levels`. This can be
 162 very handy!

163 In this example our input data consists of a data frame in which the `feeding.mode` column is
 164 already coded as a factor. In general, however, had we read this data from an input text file in, for example,
 165 comma-separated-value format, R would've created a *character* (rather than factor) formatted column
 166 by default. To adjust this we can set the argument `stringsAsFactors=TRUE` in our file-reading
 167 function, which, in that case, might be the base R function `read.csv`.

```
sunfish.feed.mode <- setNames(sunfish.data$feeding.mode,  
  rownames(sunfish.data))  
levels(sunfish.feed.mode)
```

```
## [1] "non" "pisc"
```

169 Here we see that our factor vector has two levels: "non" and "pisc". These two character levels
 170 refer to non-piscivorous and piscivorous fishes. Since R factors have no particular character limit on their
 171 levels, let's update our data to use these more descriptive names: once again using the function `levels`.
 172 `levels` is an odd R method in that it can serve both as an *extractor* function, that pulls out the levels of
 173 a factor – as well as acting as an assignment or *replacement* function, in which the levels of the factor
 174 are updated. When we adjust our factor levels for `sunfish.feed.mode`, we're using `levels` in this
 175 latter fashion.

```
levels(sunfish.feed.mode) <- c("non-piscivorous",  
  "piscivorous")  
levels(sunfish.feed.mode)
```

```
## [1] "non-piscivorous" "piscivorous"
```

177 Now we're ready to proceed and fit our models. To do so, I'll use the *phytools* function `fitMk` and fit a
 178 total of four models, as previously indicated: "ER", the equal rates model; "ARD", the all-rates-different
 179 model; and, lastly, the two different irreversible models – one in which non-piscivory can evolve to
 180 piscivory, but not the reverse; and a second in which precisely the opposite is true.

181 For these latter two irreversible models, we'll tell `fitMk` how to build the model by creating and
 182 supplying what I'll refer to as a "design matrix" for each model that we want to fit. This design matrix
 183 should be of dimensions $k \times k$, for k levels of the trait, with integer values in the positions of the matrix
 184 corresponding to allowed transitions, and zeros elsewhere. We use different non-zero integer value for
 185 each rate that we want to permit to assume a different value in our fitted model. Since our $k = 2$, this is

very easy; however, the same principle would apply to any value of k . (See Revell and Harmon 2022 for more complex examples.)

```
sunfish.ER_model<-fitMk(sunfish.tree,sunfish.feedmode,
  model="ER")
sunfish.ARD_model<-fitMk(sunfish.tree,sunfish.feedmode,
  model="ARD")
sunfish.Irr1_model<-fitMk(sunfish.tree,
  sunfish.feedmode,model=matrix(c(0,1,0,0),2,2,
  byrow=TRUE))
sunfish.Irr2_model<-fitMk(sunfish.tree,
  sunfish.feedmode,model=matrix(c(0,0,1,0),2,2,
  byrow=TRUE))
```

Having fit our four models, we can also compare them to see which is best-supported by our data. To accomplish this I'll use a generic `anova` function call. `anova` will print the results of our model comparison; however, it's important that we also assign the value returned by `anova` to a new object. In my example, I'll call this object `sunfish.aov` – but the name is arbitrary.

```
sunfish.aov<-anova(sunfish.ER_model,sunfish.Irr1_model,
  sunfish.Irr2_model,sunfish.ARD_model)
```

	##		log(L)	d.f.	AIC	weight
193	##	sunfish.ER_model	-13.07453	1	28.14906	0.3486479
194	##	sunfish.Irr1_model	-12.98820	1	27.97640	0.3800846
195	##	sunfish.Irr2_model	-14.20032	1	30.40064	0.1130998
196	##	sunfish.ARD_model	-12.86494	2	29.72987	0.1581677

This table shown above gives each of our fitted model names, their log-likelihoods, the number of parameters estimated, a value of the Akaike Information Criterion (AIC), and the Akaike model weights. Smaller values of AIC indicate better support for the corresponding model – taking into account its parameter complexity (Burnham and Anderson 2003). Model weights can be interpreted as the “weight of evidence” favoring each of our four trait evolution hypotheses (or even the probability that the model is true, given that all possible models are in our set, e.g., Link and Barker 2006).

Based on this analysis, we might conclude that the first irreversible model (`Irr1_model`), in which non-piscivory can evolve to piscivory, but not the reverse, is best supported; however, we have a very similar weight of evidence favoring the equal-rates model (`ER_model`), in which backward and forward transition rates between the two states are identical!

With the result of our `anova` call in hand (as the `sunfish.aov` object), we're ready to pass it on directly to *phytools*' new generic `simmap` method. By design, doing so will tell `simmap` to generate stochastic character maps under each of our four models with relative frequencies that are equal to the weight of evidence supporting of each model.

Here, I'll choose to sample 1,000 stochastic character maps – however, this number is somewhat arbitrary. How many is enough? Certainly one or ten are two few, and perhaps a good rule of thumb might be to ask ourselves if we're interested in trait histories that might be expected to be observed (under our model or models) in fewer than one of 100 or 1,000 realizations of the evolutionary process on our phylogeny. If not, then 100 or 1,000 stochastic maps may be enough. There's no harm in generating more, but this can require significant computational effort (depending on the size of our tree), and many empirical studies use a number of stochastic character histories that ranges on this 100 - 1,000 interval.

```
sunfish.simmap<-simmap(sunfish.aov,nsim=1000)
sunfish.simmap
```

1000 phylogenetic trees with mapped discrete characters

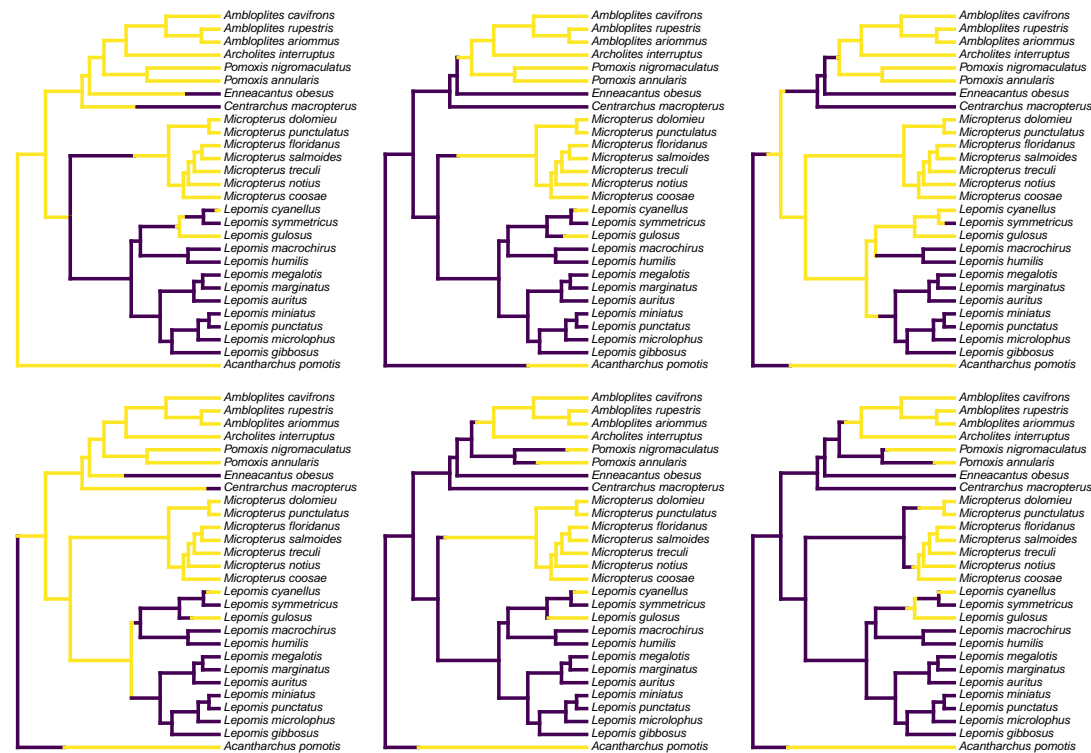


Figure 1. Six randomly chosen stochastic character maps of feeding mode (non-piscivorous, in dark blue, vs. piscivorous) on a phylogeny of 28 centrarchid fish species. Stochastic character mapping involves randomly sampling character histories that are consistent with our tip data in proportion to their probability under a model. In this case, histories were sampled under the set of four alternative Mk models of a binary trait, with relative frequencies proportional to the weight of evidence supporting each model. The tree and data are modified from Revell and Collar (2009). See main text for additional details.

219 If we preferred, we could've generated stochastic character maps for just the best-supported of our
220 four models. Using the `simmap` generic method, this would be done either by supplying our `anova`
221 result and setting the optional argument `weighted=FALSE` – or simply by passing our favored Mk
222 model directly to the function!

223 In spite of the significant number of stochastic simulations involved, this analysis should run fairly
224 quickly (obviously, depending on the speed of our computer). In part this is because we saved computation
225 time by circumventing the need to re-estimate our Mk transition matrix, **Q**, separately for each sampled
226 model. An additional advantage of this approach is that it's also allowed us to (partly) account for variation
227 in our modeled process of evolution that's due to uncertainty in model selection.

228 Figure 1 shows a set of six, randomly chosen stochastic character histories for our trait (feeding mode)
229 on our input tree. Readers should see that each of these are consistent with our observed value of the
230 binary trait at the tips of the tree, but that each differs one from the other in the specific hypothesis of trait
231 evolution that it represents.

```
cols<-setNames(viridisLite::viridis(n=2),
  levels(sunfish.feedmode))
par(mfrow=c(2,3))
plot(sample(sunfish.simmap,6),ftype="i",fsize=0.6,
  colors=cols,offset=0.2)
```

232 To create my color palette for plotting I used another contributed R package that we haven't seen
233 yet called `viridisLite` by Garnier et al. (2022). `viridisLite` implements a color palette (known as the
234 "viridis" palette and originally devised by van der Walt and Smith 2015) that was designed to be both

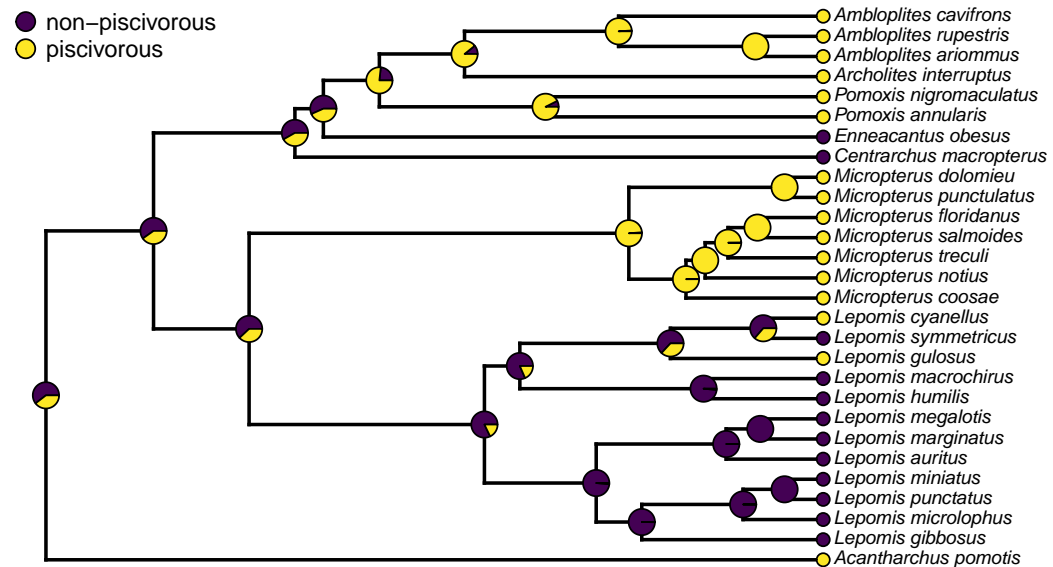


Figure 2. Posterior probabilities at each ancestral node of the centrarchid tree of Figure 1 from stochastic character mapping using model weights to sample across four different extended Mk trait evolution models. See main text for more details.

attractive and colorblind-friendly. To replicate Figure 1 exactly, users should first install *viridisLite* from CRAN by running `install.packages("viridisLite")` – but they do not need to load it. Calling the contributed package function using the double colon syntax, `::`, takes care of that (i.e., `viridisLite::viridis`).

Although Figure 1 already gives us a general sense of the uncertainty of our ancestral character history on the tree for our trait, most commonly we don't want to simply graph a subset (or all) of our stochastically mapped trees. Typically, instead, we'd first summarize our stochastic character maps (in multiple ways), and then proceed to plot or analyze these summarized findings.

Often, *phytools* users undertaking stochastic character mapping will compute the posterior probabilities of each value of the character trait at each internal node of the tree, which one can obtain by simply *counting* the fraction of stochastic maps for which each node is in each of the observed states of our character trait. These values correspond to a form of ancestral state estimation, giving us an approximation of the marginal probabilities that each hypothetical ancestor at each node of the tree was in each of our observed states. We've conditioned on our transition model and its Maximum Likelihood parameter estimates – although in this instance we also *integrate* across a set of four evolutionary models in proportion to the weight of evidence in support of each one. In *phytools*, these values marginal posterior probabilities can be obtained using the generic `summary` method for our object class, which is then easily plotted as follows.

```
plot(summary(sunfish.simmmap), ftype="i", fsize=0.7,
      colors=cols, cex=c(0.6, 0.3))
legend("topleft", levels(sunfish.feed.mode), pch=21,
      pt.cex=1.5, pt.bg=cols, bty="n", cex=0.8)
```

A correct interpretation of the graph of Figure 2 is that it shows the observed discrete character states (at the tips of the tree) and the posterior probabilities from stochastic mapping that each internal node is in each state – all while integrating over our four different transition models in proportion to the weight of evidence for each model!

In addition to node probabilities, *phytools* users undertaking a stochastic character mapping analysis are often interested in the number of changes of each type that are implied by the evolutionary process and our data. The procedure of stochastic mapping samples full character histories (not just states or probabilities at nodes) and can thus be deployed to produce estimates of the posterior probability

distribution of the character changes of each type on specific edges, in specific clades, or across the entire phylogeny, conditioning on our sampled model or models.

To obtain these distributions, we'll first call the generic method `density` which (when applied to an object from stochastic mapping) computes the relative frequency distribution of changes of each type over the whole tree. We can then proceed to graph our results using a different generic `plot` method, as follows. Remember, our character is binary, so there are only two types of character state changes: from non-piscivorous \rightarrow piscivorous, and the reverse.

```
sunfish.density<-density(sunfish.simap)
sunfish.density

##
## Distribution of changes from stochastic mapping:
## non-piscivorous->piscivorous      piscivorous->non-piscivorous
## Min.      :0      Min.      :0
## Median    :5      Median    :2
## Mean      :4.13     Mean      :2.24
## Max.      :10     Max.      :9
##
## 95% HPD interval(non-piscivorous->piscivorous): [0, 8]
## 95% HPD interval(piscivorous->non-piscivorous): [0, 6]

par(mfrow=c(1,2),las=1,cex.axis=0.7,cex.lab=0.8)
COLS<-setNames(cols[2:1],sunfish.density$trans)
plot(sunfish.density,ylim=c(0,0.6),
      transition=names(COLS)[1],colors=COLS[1],main="")
mtext("a) transitions to piscivory",line=1,adj=0,
      cex=0.8)
plot(sunfish.density,ylim=c(0,0.6),
      transition=names(COLS)[2],colors=COLS[2],main="")
mtext("b) transitions to non-piscivory",line=1,adj=0,
      cex=0.8)
```

The distributions shown in Figure 3 give the relative frequencies of changes of each type across our set of mapped histories, as well as Bayesian 95% high probability density (HPD) intervals calculated using the R package *coda* (Plummer et al. 2006). For a binary trait like that of this example (and thus with only two types of transitions), we could have instead overlain the distributions of backwards and forwards transitions in character state in a single plot panel. In this particular instance, however, I found that overplotting the two different distributions resulted in a figure that was too difficult to read, and preferred instead to show the distributions in separate panels as in Figure 3. For multistate characters with more than two types of changes between states, the same `plot` method will produce a $k \times k$ matrix of figure panels, each i,j th panel of which will contain the posterior distribution of changes from character state i to j .

An interesting attribute of the character state change distributions for this centrarchid feeding mode analysis is that they are both markedly bi-modal. This is due, in part, to our specific procedure of model-averaging in which we sampled both reversible and irreversible character evolution models in proportion to their weights, and isn't something we would've seen had we chosen to analyze just one model or the other. (Recall that the weight of evidence was highly similar between our equal-rates model and the irreversible model in which piscivory is acquired from non-piscivory, but never the reverse. See above.) This pattern is also appropriately captured by the broad HPD intervals on each of the two types of transitions.

Lastly, in addition to these analyses, *phytools* also makes it quite straightforward to visualize the posterior probabilities of each of the two trait conditions not only at nodes, but also also along the branches of the phylogeny. This is accomplished using the *phytools* function `densityMap` (Revell 2013), which creates a graph showing the probability density of stochastic histories in each of our mapped states. By

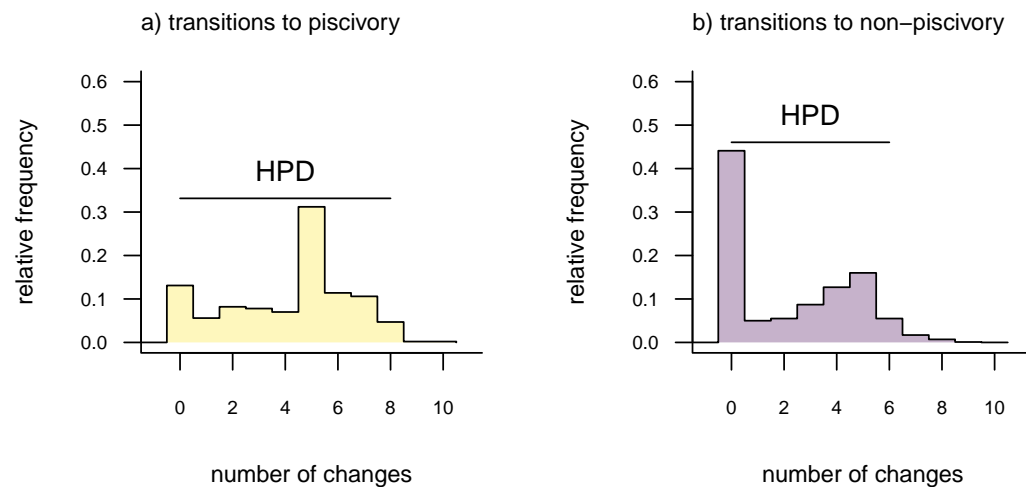


Figure 3. Posterior probability distributions of changes from either a) non-piscivory to piscivory, or b) piscivory to non-piscivory, obtained from an analysis of stochastic mapping. HPD indicates the 95% high probability density interval for changes of each type. See main text for additional details.

design, in *phytools* this object can be first created (using the `densityMap` function), updated (using the method `setMap` to adjust our color palette for plotting), and then graphed (using a generic `plot` method that was created for this specific object class). I'll illustrate this set of procedures in the following code block.

```
sunfish.densityMap<-densityMap(sunfish.simmap,plot=FALSE,
                               res=1000)
sunfish.densityMap
```

```
## Object of class "densityMap" containing:
##
## (1) A phylogenetic tree with 28 tips and 27 internal nodes.
##
## (2) The mapped posterior density of a discrete binary character
##      with states (non-piscivorous, piscivorous).
```

```
sunfish.densityMap<-setMap(sunfish.densityMap,
                           viridisLite::viridis(n=10))
plot(sunfish.densityMap,lwd=3,outline=TRUE,
     fsize=c(0.6,0.7),legend=0.1)
```

Having enthusiastically demonstrated the model-averaging feature of the new *phytools* `simmap` method, I'd be remiss if I failed to note that this is *not* (as yet) the standard workflow for ancestral state reconstruction of discrete characters in general, nor for stochastic mapping in particular. More typically, researchers select the best model and then proceed to hold this model (and its parameters) constant through subsequent calculations (e.g., Yang 2014), or they sample parameter values for a single model from their joint posterior distribution using MCMC (e.g., shown in Revell and Harmon 2022). I think, however, that there is a very strong case to be made that if, for example, 51% of the weight of evidence points to a model in which a specific node has a high conditional probability of being in state *a*, while 49% of the weight of evidence points to a model wherein the same node has a high probability of being in state *b*, then the correct marginal probability that the node is *actually* in state *a* is probably closer to 0.5 than

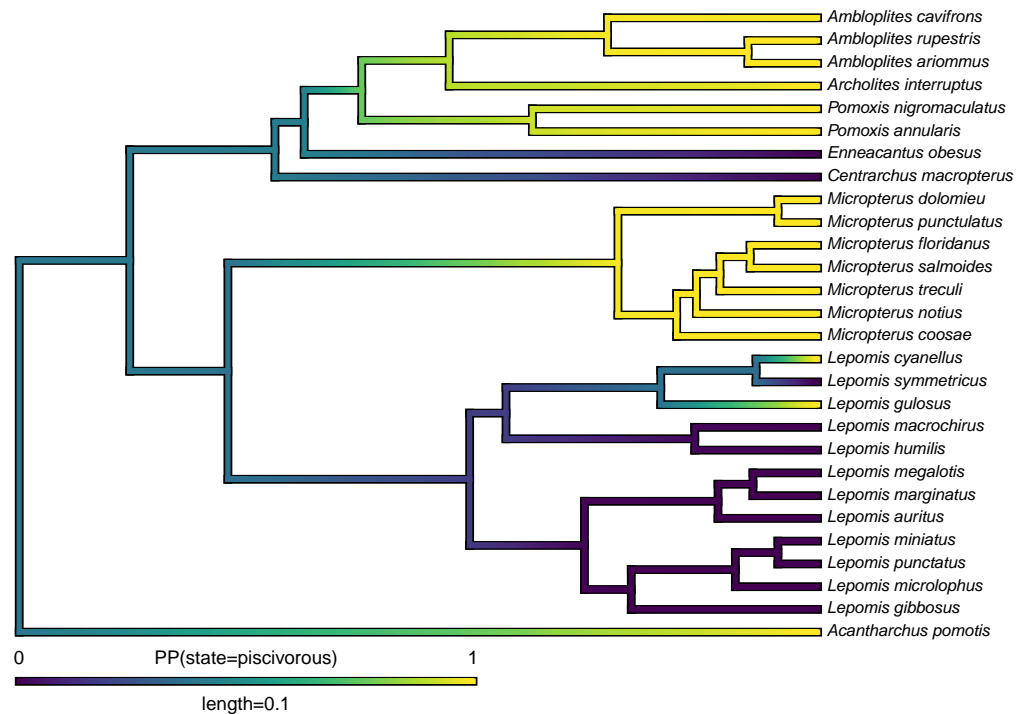


Figure 4. Posterior probability density of each of the two character levels, piscivory and non-piscivory, based on stochastic character mapping, graphed along the edges of a tree of centrarchid fishes using a color gradient. See main text for more details.

320 1.0. Indeed, this would be our exact interpretation of this result if we consider the model weights as the
 321 probability that each model is correct (assuming that all possible models are in our set, e.g., Link and
 322 Barker 2006).

323 Apart from the analyses shown, stochastic mapping as implemented in *phytools* is a very flexible
 324 method via which we might sample the matrix of transition rates from its posterior distribution under
 325 a model, incorporate uncertainty in the character state values for different species, take into account
 326 polymorphic character conditions and hidden-rates of trait evolution, and integrate over phylogenetic
 327 uncertainty. A comprehensive survey of this functionality is beyond the scope of the present article;
 328 however, considerable additional information about stochastic mapping in R can be found in the *phytools*
 329 documentation pages as well as elsewhere online.

330 4.2 The polymorphic trait evolution model

331 Another important, but much more recently-added, tool in the *phytools* R package is a method (called
 332 *fitpolyMk*) that's designed to fit a discrete character evolution model to trait data containing intraspe-
 333 cific polymorphism (Revell and Harmon 2022). In this case, our model is one in which an evolutionary
 334 transition from (say) character state *a* to character state *b* must first pass through the intermediate poly-
 335 morphic condition of *a + b*. This model starts off very simply – but will become increasingly complicated
 336 for increasing numbers of monomorphic conditions of our trait. Not only that, but as soon as we have
 337 more than two monomorphic states, we must also consider whether our character is evolving in an ordered
 338 (Figure 5a) or unordered (Figure 5b) fashion (Revell and Harmon 2022). Figure 5 shows the general
 339 structure of an ordered and unordered polymorphic trait evolution model – both for the same, underlying
 340 number of monomorphic conditions of our trait (four).

```
par(mfrow=c(1, 2))
graph.polyMk(k=4, ordered=TRUE, states=0:3,
mar=rep(0.1, 4))
```

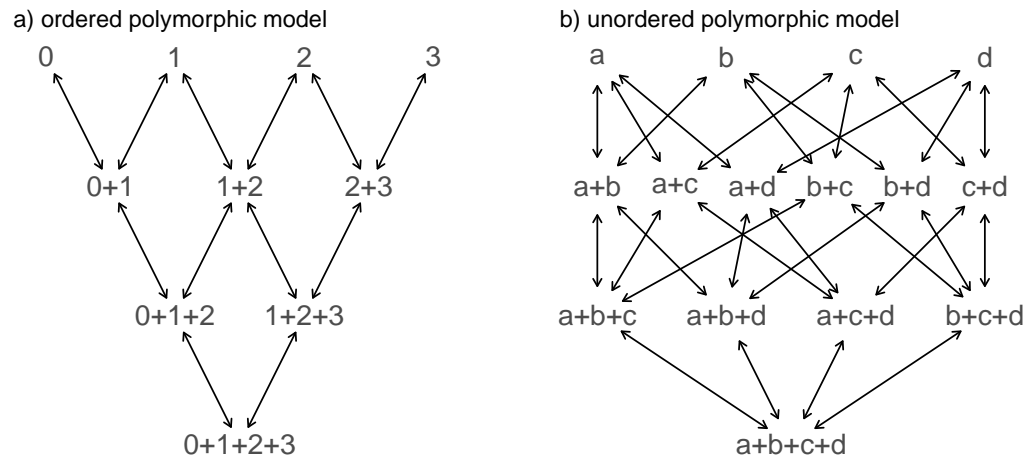


Figure 5. Example structures of two alternative polymorphic trait evolution models for characters with four monomorphic conditions: a) an ordered model with states 0 to 3; b) an unordered model, with states *a*, *b*, *c*, and *d*. The maximum parameter complexity of each model corresponds to $2 \times$ the number of double-ended arrows in the panel. See main text for additional details.

```
mtext("a) ordered polymorphic model", line=-1, adj=0.2,
      cex=0.8)
graph.polyMk(k=4, ordered=FALSE, states=letters[1:4],
             mar=rep(0.1, 4), spacer=0.15)
mtext("b) unordered polymorphic model", line=-1,
      adj=0.2, cex=0.8)
```

Obviously, the potential parameter complexity of the unordered polymorphic trait evolution model is higher than the ordered model. Since there exists an unordered model that also has all ordered models as a special case, ordered and unordered models can be compared using likelihood-ratio tests (if nested) or information criteria.

To try out our polymorphic trait evolution model, let's use an excellent, recently-published dataset from Halali et al. (2020) consisting of a phylogenetic tree containing 287 *Mycalesina* butterfly species and data for butterfly habitat use. Halali et al. (2020) coded habitat as a polymorphic trait in which, for example, a species using both "forest" and forest "fringe" habitat would be recorded as "forest+fringe". In this case, our polymorphic trait evolution model will assume that to evolve from forest specialization to fringe specialization, a species must first (at least transiently) evolve through the polymorphic condition of using both habitats at once. This seems logical.

The Halali et al. (2020) dataset and tree now come packaged with the *phytools* library, so both can be loaded using the `data` function, just as we saw for the centrarchid data and tree of our previous example.

```
data(butterfly.tree)
data(butterfly.data)
```

Let's begin by inspecting our data.

```
head(butterfly.data)
```

```
##          habitat
## Myc_francisca_formosana? forest+fringe+open
## Bic_cooksoni         open
## Bic_brunnea          forest
## Bic_jefferyi         fringe+open
```

```
360 ## Bic_auricruda_fulgida          forest
361 ## Bic_smithi_smithi              forest+fringe
```

362 `fitpolyMk` requires us to separate the different states in each polymorphic condition using the +
 363 symbol, but does not demand that our states be ordered in a consistent manner. In other words, a+b and
 364 b+a would be considered (properly) to be same polymorphic condition! As a first preliminary step in
 365 our analysis, we can proceed to extract the column of habitat use data (`habitat` in our data frame) as a
 366 vector, and then print the different levels that it takes.

```
butterfly.habitat<-setNames(butterfly.data$habitat,
  rownames(butterfly.data))
print(levels(butterfly.habitat))
```

```
367 ## [1] "forest"          "forest+fringe"      "forest+fringe+open"
368 ## [4] "fringe"          "fringe+open"        "open"
```

369 Now, let's proceed to fit our polymorphic trait evolution model to these data. In this instance, I'll
 370 fit a grand total of six different models. This isn't a comprehensive set of the conceivable models for
 371 polymorphic data with these levels, but it seemed like a reasonable selection for illustrative purposes.

372 The first three of these models all suppose that the evolution of my discrete character is totally
 373 unordered. Among this set, we'll imagine, first, equal transition rates between all monomorphic states
 374 or polymorphic conditions. For our second model, we'll permit all possible transition rates between
 375 states or state combinations to assume *different* values. Finally, for our third model we'll assume that
 376 the acquisition of polymorphism (or its increase) occurs with one rate, whereas the loss (or decrease) of
 377 polymorphism occurs with another, separate rate. We refer to this last scenario as the "transient model"
 378 following Revell and Harmon (2022). This name for the model comes from the general notion that
 379 if the rate of loss exceeds the rate of gain, then polymorphism will typically be relatively transient in
 380 nature. Since polymorphism tends to be less frequently observed in the types of data that typify many
 381 phylogenetic comparative studies, including this model in our set seems like a reasonable idea.

382 To get our remaining three models, and reach the six total models that I promised at the outset of this
 383 section – for each of the three listed above in which character evolution is unordered, we'll simply add a
 384 second *ordered* model in which we assume that character evolution for our three monomorphic conditions
 385 tends to proceed as follows: *forest* ↔ *fringe* ↔ *open* – not forgetting, of course, about the intermediate
 386 polymorphic conditions found between each pair of monomorphic states!

387 To fit our first three models in R, we'll use the function `fitpolyMk` from the *phytools* package as
 388 follows.

```
butterfly.ERunordered<-fitpolyMk(butterfly.tree,
  butterfly.habitat,model="ER")
```

```
389 ##
390 ## This is the design matrix of the fitted model.
391 ## Does it make sense?
392 ##
393 ##               forest fringe open
394 ## forest               0      0   0
395 ## fringe               0      0   0
396 ## open                 0      0   0
397 ## forest+fringe        1      1   0
398 ## forest+open          1      0   1
399 ## fringe+open          0      1   1
400 ## forest+fringe+open    0      0   0
401 ##               forest+fringe forest+open fringe+open
402 ## forest               1              1              0
403 ## fringe               1              0              1
404 ## open                 0              1              1
```

```

405 ## forest+fringe          0          0          0
406 ## forest+open            0          0          0
407 ## fringe+open            0          0          0
408 ## forest+fringe+open     1          1          1
409 ##                        forest+fringe+open
410 ## forest                  0
411 ## fringe                  0
412 ## open                    0
413 ## forest+fringe          1
414 ## forest+open            1
415 ## fringe+open            1
416 ## forest+fringe+open     0

```

By default, `fitpolyMk` begins by printing out the design matrix of the model for us to verify. The design matrix is of dimensions dictated by the number of states and polymorphic conditions of our character, with integers populating the different types of transitions, from row to column, that should be permitted under our model – and zeros indicating disallowed transition types. The specific integer values don’t mean anything; however, different integer values imply that the corresponding transitions will be allowed to take place with different rates under our model.

This can be helpful, because we should find that it corresponds with the design matrix that was discussed under the simpler `Mk` model of the previous section – as well as with the graphed models of Figure 5. If we don’t want the design matrix to print, though, we can turn off this behavior simply by setting the optional argument `quiet=TRUE`. Let’s do that for our remaining two unordered models.

```

butterfly.ARD_unordered<-fitpolyMk(butterfly.tree,
  butterfly.habitat,model="ARD",quiet=TRUE,
  opt.method="optimParallel",rand.start=TRUE)
butterfly.transient_unordered<-fitpolyMk(
  butterfly.tree,butterfly.habitat,
  model="transient",quiet=TRUE,
  opt.method="optimParallel",rand.start=TRUE)

```

Astute readers may notice that I added two additional arguments that didn’t feature in my previous `fitpolyMk` function call: `opt.method="optimParallel"` and `rand.start=TRUE`. The former tells my optimizer to use the *optimParallel* package (Gerber and Furrer 2019) for optimization. The latter says “choose random starting values.” Both of these, and sometimes multiple optimization replicates, may be required to find our Maximum Likelihood solution for these complex models. In fact, I virtually guarantee it!

Now we can proceed to do the same thing, but this time updating the argument value `ordered` to `ordered=TRUE`. When we switch from fitting an unordered polymorphic trait evolution model to our ordered model, it suddenly becomes critical that we specify the order levels using the optional function argument `order`. If `order` isn’t indicated, `fitpolyMk` will simply assume that our characters are ordered alphanumerically – but this is very rarely likely to be correct! (By chance, it happens to be true of our butterfly dataset. I assigned the argument `order` anyway, just to be safe.)

```

levs<-c("forest","fringe","open")
levs

```

```

439 ## [1] "forest" "fringe" "open"

```

```

butterfly.ER.ordered<-fitpolyMk(butterfly.tree,
  butterfly.habitat,model="ER",ordered=TRUE,order=levs,
  quiet=TRUE)
butterfly.ARD.ordered<-fitpolyMk(butterfly.tree,
  butterfly.habitat,model="ARD",ordered=TRUE,

```



```
order=levs, quiet=TRUE, opt.method="optimParallel",
rand.start=TRUE)
butterfly.transient.ordered<-fitpolyMk(butterfly.tree,
butterfly.habitat, model="transient", ordered=TRUE,
order=levs, quiet=TRUE, opt.method="optimParallel",
rand.start=TRUE)
```

440 Now, with all six models in hand, let's compare them using an anova call as follows. I'll save my
441 results from our model comparison to the object butterfly.aov.

```
butterfly.aov<-anova(butterfly.ER.ordered,
butterfly.ER.unordered,
butterfly.transient.ordered,
butterfly.transient.unordered,
butterfly.ARD.ordered,
butterfly.ARD.unordered)
```

```
442 ##               log(L) d.f.      AIC      weight
443 ## object          -329.0390    1 660.0779 1.472873e-09
444 ## butterfly.ER_unordered -355.8122    1 713.6244 3.472845e-21
445 ## butterfly.transient_ordered -329.0205    2 662.0409 5.519508e-10
446 ## butterfly.transient_unordered -353.4496    2 710.8991 1.356691e-20
447 ## butterfly.ARD_ordered -297.7376   12 619.4753 9.658773e-01
448 ## butterfly.ARD_unordered -295.0807   18 626.1614 3.412273e-02
```

449 A quick word of caution to readers is probably merited here. These models can be quite difficult to
450 optimize, meaning that it's not inconceivable to imagine that (in spite of our best efforts) fitpolyMk
451 hasn't converged on the true Maximum Likelihood solution for one model or another. Although the true
452 best solution may be unknowable (this is why we use numerical optimization to try and ascertain it),
453 common sense can be a valuable defense against very obvious failures of optimization. For instance,
454 had we found that the most complex model (in our case, butterfly.ARD.unordered) had a lower
455 likelihood than any of its nested counterparts (for instance, butterfly.ARD.ordered), this would
456 give us very strong cause to believe that one or both models hadn't converged, and that we should perhaps
457 try different random starts or alternative optimization routines to try to find better solutions!

458 Nonetheless, taking our fitted models at face value, model comparison shows that (among the models
459 in our set) the best supported by far (accounting for parameter complexity) is the ordered, all-rates-different
460 model. phytools has a function to graph this model, so let's go ahead and use it!

```
plot(butterfly.ARD.ordered, asp=0.65, mar=rep(0.1, 4),
cex.traits=0.8)
legend("bottomleft", legend=c(paste("log(L) =",
round(logLik(butterfly.ARD.ordered), 2)),
paste("AIC =", round(AIC(butterfly.ARD.ordered), 2))),
bty="n", cex=0.8)
```

461 Just as with our fitted Mk models from the prior section, we can also pass this model object to
462 our generic stochastic character mapping method, simmap. When we do, simmap will automatically
463 generate a set of 100 stochastic character maps under our fitted model. We could've likewise passed
464 simmap our anova results, just as we did with our "fitMk" objects in the centrarchid example, above.
465 In this case, however, nearly all the weight of evidence fell on one model, so this wouldn't really make
466 much difference anyway.

```
butterfly.simmap<-simmap(butterfly.ARD.ordered)
butterfly.simmap
```

```
467 ## 100 phylogenetic trees with mapped discrete characters
```

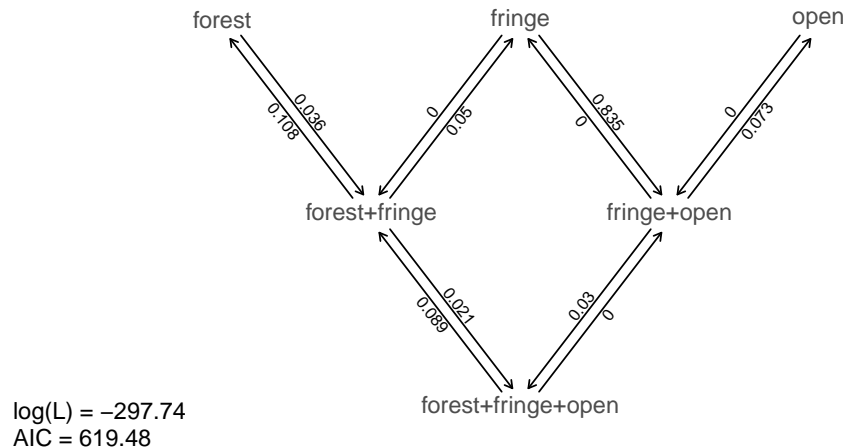


Figure 6. Best-fitting polymorphic trait evolution model for the evolution of habitat use in *Mycalesina* butterflies. Data and phylogeny are from Halali et al. (2020). See main text for more details.

Now that we have our stochastically mapped trees, let's compute a summary, just as we did in the prior section.

```
butterfly.summary<-summary(butterfly.simap)
```

Much as we saw earlier, the object from our generic `summary` call can be conveniently plotted using *phytools*. In this case, rather than using the *viridis* palette we saw earlier, I'll use the base graphics function `rgb` to attempt to select colors for plotting that are evenly spaced in a red-green-blue color space in which the "corners" (red, green, and blue) correspond to the three monomorphic states of our data. Does that make sense? I'm colorblind, so it's hard for me to be sure how the `rgb` color space captures the "intermediacy" of the polymorphic conditions between the corresponding monomorphic states. Nonetheless, I hope the reader can use this demonstration as an *example* of how to specify custom palettes, rather than an endorsement of a specific palette!

```
hab.cols<-setNames(c(rgb(0,1,0),rgb(0,0.5,0.5),
  rgb(1/3,1/3,1/3),rgb(0,0,1),rgb(0.5,0.5,0),
  rgb(1,0,0)),levels(butterfly.habitat))
par(fg="transparent")
h<-max(nodeHeights(butterfly.tree))
plot(butterfly.summary,type="arc",ftype="off",
  colors=hab.cols,cex=c(0.4,0.2),part=0.5,lwd=1,
  arc_height=0.4,ylim=c(-3,35))
par(fg="black")
legend("topleft",names(hab.cols),pch=21,pt.bg=hab.cols,
  pt.cex=1.5,cex=0.8,bty="n")
axis(1,pos=-1,at=h-seq(0,h,by=5)+0.4*h,
  labels=seq(0,h,by=5),cex.axis=0.8)
axis(1,pos=-1,at=-h+seq(0,h,by=5)-0.4*h,
  labels=seq(0,h,by=5),cex.axis=0.8)
```

Excellent! Figure 7 shows both the observed (at the tips) and reconstructed (at the internal nodes) marginal posterior probabilities for each of our states and polymorphic conditions.

Lastly, let's graph the posterior distribution of the accumulation of lineages in each state over time, using the *phytools* function `ltt` as follows. We can even do this while retaining the same color palette as we used for Figure 7. (We'll learn more about `ltt` in a subsequent section.) The resultant plot in

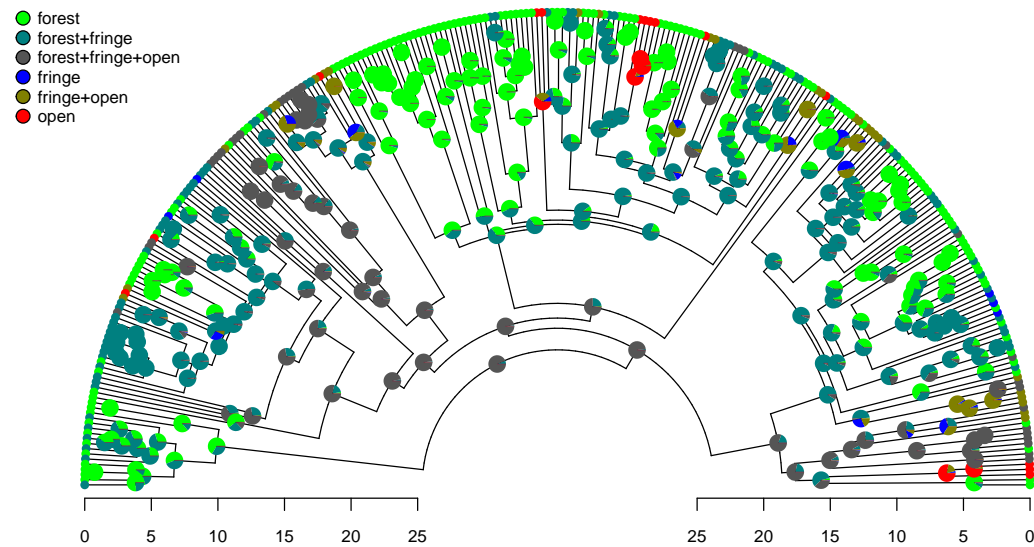


Figure 7. Posterior probabilities of monomorphic or polymorphic conditions at internal nodes from stochastic mapping under an ordered, ARD polymorphic model of trait evolution. Data and phylogeny are from Halali et al. (2020). The horizontal axis is in millions of years before the present. See main text for additional details.

Figure 8 simultaneously shows not only the accumulation of lineages in each mono- or polymorphic state, but also the variation attributable to uncertainty in the evolutionary history of our group from our stochastic character maps! Even though Figure 8 looks very cool – to be fair, this type of graph is only especially meaningful for the situation in which the taxa of our phylogeny have been completely or close to completely sampled. In this example, we have around 85% of described species for the group (Halali et al. 2020) – a high enough sampling fraction, perhaps, to make this plot meaningful. Sampling fractions in phylogenetic comparative biology, however, are often much lower!

```
butterfly.ltt<-ltt(butterfly.simmmap)
par(mar=c(4.1,4.1,1.1,1.1))
plot(butterfly.ltt,show.total=FALSE,bty="n",las=1,
      cex.axis=0.7,cex.lab=0.8,colors=hab.cols)
```

As with stochastic mapping under the standard *Mk* model, implementation of the polymorphic trait evolution model in *phytools* also allows us to take into account uncertainty in the data or in the phylogeny as well as variation in the rate of evolution between different clades and branches of the tree under the hidden rates model of Beaulieu et al. (2013, also see below). Covering all of this functionality here is not possible; however, additional information is available via *phytools* documentation pages and online.

4.3 Hidden rate models

In addition to *fitpolyMk*, another relatively recent addition to the *phytools* package for discrete character analysis has been the function *fitHRM*. *fitHRM* implements the hidden-rates trait evolution model of Marazzi et al. (2012) and Beaulieu et al. (2013). Under this model, which is closely related to the covarion model from phylogenetic inference (Galtier 2001; Penny et al. 2001), each observed state of our discrete trait may have one or more unobserved levels. These different hidden trait levels are each free, in turn, to possess different rates of transition to the other observed character conditions in our trait space. An important aspect of this model it allows us to explicitly capture heterogeneity in the evolutionary process of trait evolution – not only between different observed conditions of our character, but also across different branches and clades of the phylogeny (e.g., Beaulieu et al. 2013; King and Lee 2015). Note that both hidden-rate models and ancestral character estimation, which we'll see more of below, are also implemented in the excellent *corHMM* package of Beaulieu et al. (2022).

To illustrate use of the hidden-rates model in *phytools*, we can load a phylogenetic tree of lizards

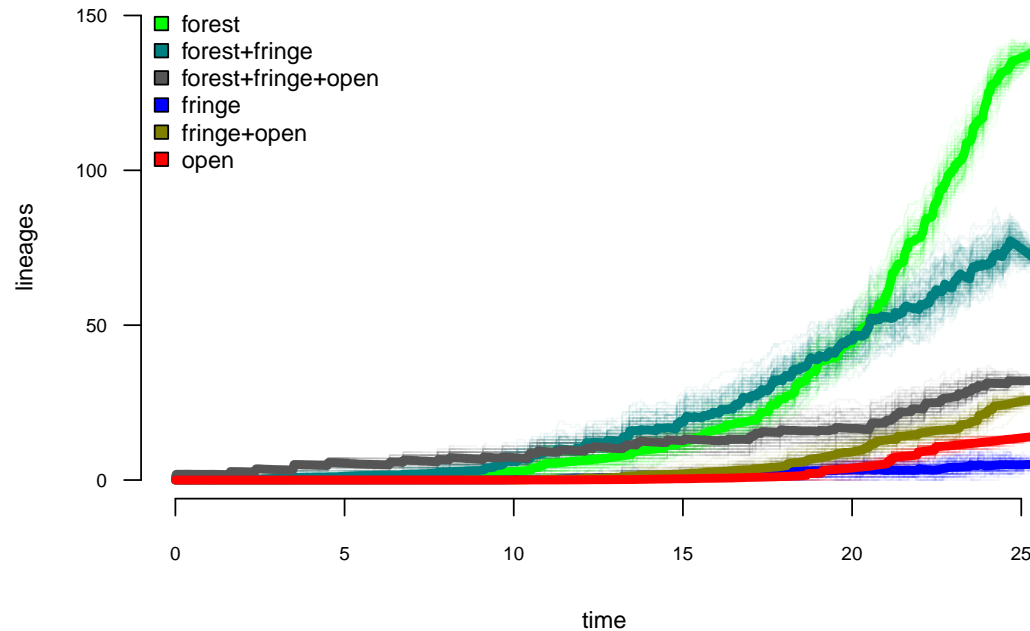


Figure 8. Lineage-through-time plot showing the reconstructed accumulation of lineages in each polymorphic condition or monomorphic state over time, from 100 stochastic character maps. Data and phylogeny are from Halali et al. (2020). See main text for additional details.

508 from the diverse South American family Liolaemidae, along with a dataset for parity mode (oviparity
509 vs. viviparity) and different environmental trait measures. Both the phylogeny and the trait data were
510 obtained from Esquerré et al. (2019) and, like the other datasets used in this article, are now packaged
511 with the *phytools* R library.

```
data(liolaemid.tree)
data(liolaemid.data)
```

512 We can start by inspecting our data object.

```
head(liolaemid.data)
```

```
513 ##          parity_mode max_altitude temperature
514 ## Ctenoblepharys_adspersa          O          750          23.05
515 ## Liolaemus_abaucan              O          2600          20.20
516 ## Liolaemus_albiceps             V          4020          12.38
517 ## Liolaemus_andinus              V          4900          11.40
518 ## Liolaemus_annectens            V          4688           5.10
519 ## Liolaemus_anomalus             O          1400          23.78
```

520 We should see that the two levels of our discrete character of interest, parity mode, have been coded as
521 "O" (oviparity) and "V" (viviparity), respectively. To proceed and use *fitHRM* to fit hidden-rate models
522 with *phytools*, we must next extract the parity mode of our liolaemid species. An easy way to do that, as
523 we've seen in prior sections, is via the handy function *setNames*.

```
liolaemid.parity<-setNames(liolaemid.data$parity_mode,
                             rownames(liolaemid.data))
```

524 One flavor of hidden-rates model, as described in Revell and Harmon (2022, in which we call it the
525 "umbral" model, from *umbral* meaning threshold in Spanish), allows transitions only between specific,

labile conditions of the trait. Transitions in observed state are not permitted, on the other hand, any time a lineage finds itself in the hidden, inert level. (This model is also closely related to what was referred to as the “pre-cursor model” by Marazzi et al. 2012.) Let’s try to fit this model to our data using *two* rate categories per observed state of our character. This is specified using the function argument `ncat=2`. (We could have chosen to model more than two levels per observed trait value, or even a different number of levels for the “O” and “V” conditions, respectively.)

Since this model class can be quite difficult to fit to data, `fitHRM` is designed to use multiple optimization iterations (10 by default, but this can be adjusted by modifying the optional function argument `niter`) with different random starting values. These optimization iterations can also be parallelized across our computer cores by specifying `parallel=TRUE`. Just as was true of `fitMk` and `fitpolyMk`, optimization in `fitHRM` can *also* be parallelized using *optimParallel* (Gerber and Furrer 2019) – however, we must not try to set `parallel=TRUE` and `opt.method="optimParallel"` at the same time!

```
liolaemid.hrm<-fitHRM(liolaemid.tree,liolaemid.parity,
  ncat=2,umbral=TRUE,pi="fitzjohn",parallel=TRUE)
```

Does it make sense?

```

541      O O* V V*
542 O  0  1  2  0
543 O*  3  0  0  0
544 V   4  0  0  5
545 V*  0  0  6  0
```

Opened cluster with 10 cores.

Running optimization iterations in parallel.

Please wait....

Much as we saw with `fitpolyMk`, by default `fitHRM` starts by printing the model design matrix to screen for users to inspect. This default setting can be turned off using `quiet=TRUE`.

Let’s review our fitted model.

```
liolaemid.hrm
```

```

553 ## Object of class "fitHRM".
554 ##
555 ## Observed states: [ O, V ]
556 ## Number of rate categories per state: [ 2, 2 ]
557 ##
558 ## Fitted (or set) value of Q:
559 ##      O      O*      V      V*
560 ## O  -1.431683  0.000000  1.431683  0.000000
561 ## O*  0.041029 -0.041029  0.000000  0.000000
562 ## V   2.267185  0.000000 -2.812138  0.544953
563 ## V*  0.000000  0.000000  0.000000  0.000000
564 ##
565 ## Fitted (or set) value of pi:
566 ##      O O* V V*
567 ##      0  1  0  0
568 ## due to treating the root prior as (a) nuisance.
569 ##
570 ## Log-likelihood: -59.117373
571 ##
572 ## Optimization method used was "optim"
573 ##
574 ## R thinks it has found the ML solution.
```


The structure of the transition matrix \mathbf{Q} ought to match our design matrix in that optimized transition rates should *only* be found in matrix cells populated by non-zero integers in our printed design. (Except for the matrix diagonal which always contains a value equal to the negative row sum, OMeara 2012; Revell and Harmon 2022.) Here we see that it does – although some Maximum Likelihood transition rate values, such as the transition rate from \circ (the labile condition of oviparity) to \circ^* (the inert condition) are not different from zero in the fitted model (also see Figure 9).

A conventional analysis workflow would typically involve comparing this fitted model to a standard Mk model (discussed above, also see Harmon 2019), as well as, perhaps, other variants of the hidden-rates model (Beaulieu et al. 2013; Revell and Harmon 2022). Here, I'll compare our umbral model to both a standard extended Mk model with different backward and forward rates of transitions (the "ARD" model), as well as to a slightly more complex hidden-rates model in which transitions *are* allowed between the hidden condition levels, just at different rates. We could fit the Mk model using the *phytools* function `fitMk`, as we did earlier – but here I'll do it using `fitHRM` by setting `ncat` (the number of rate categories for each level of the trait) to `ncat=1`. This also helps us see that standard Mk models are special cases of the hidden-rates model – just without hidden rate categories!

```
liolaemid.mk<-fitHRM(liolaemid.tree,liolaemid.parity,
  ncat=1,pi="fitzjohn",parallel=TRUE,quiet=TRUE)
liolaemid.full<-fitHRM(liolaemid.tree,liolaemid.parity,
  ncat=2,pi="fitzjohn",parallel=TRUE,quiet=TRUE)
anova(liolaemid.mk,liolaemid.hrm,liolaemid.full)
```

		log(L)	d.f.	AIC	weight
##	object	-64.27046	2	132.5409	0.21754700
##	liolaemid.hrm	-59.11737	6	130.2347	0.68917781
##	liolaemid.full	-59.11732	8	134.2346	0.09327518

By comparing these three models we see that there is relatively little support for the extended Mk ("ARD") model and for the full hidden-rates model, compared to our best-supported model: the original, umbral model. Indeed, the full hidden-rates model actually has virtually the same likelihood as our umbral model, but with two additional parameters to be estimated!

phytools now makes it very easy to undertake joint or marginal ancestral state reconstruction (e.g., Yang 2014; Revell and Harmon 2022) under a hidden-rate model, as well as under other models we've seen in this article (such as the standard extended Mk model and the polymorphic trait evolution model) via the *phytools* generic method `ancr`. Much as with the `simmap` method described previously, all we need to do is pass our fitted model object to the method, and `ancr` will do the rest. Although I won't show it here, `ancr` is also capable of computing model-averaged ancestral states if we simply supply it with a set of models (in lieu of a single model) in the form an object computed using an `anova` method call. It can also perform *joint* reconstruction, rather than the marginal ancestral state estimation shown here. (For more information on the difference between marginal and joint ancestral state estimation for discrete characters, see Yang 2014; Revell and Harmon 2022.)

```
liolaemid.hrm.asr<-ancr(liolaemid.hrm,tips=TRUE)
print(liolaemid.hrm.asr,printlen=12)
```

```
## Marginal ancestral state estimates:
##           O           O*           V V*
## 258 0.000000 1.000000 0.000000 0
## 259 0.000000 1.000000 0.000000 0
## 260 0.000000 1.000000 0.000000 0
## 261 0.000000 1.000000 0.000000 0
## 262 0.000000 1.000000 0.000000 0
## 263 0.000000 1.000000 0.000000 0
## 264 0.000000 1.000000 0.000000 0
## 265 0.000000 1.000000 0.000000 0
## 266 0.000025 0.999967 0.000009 0
```

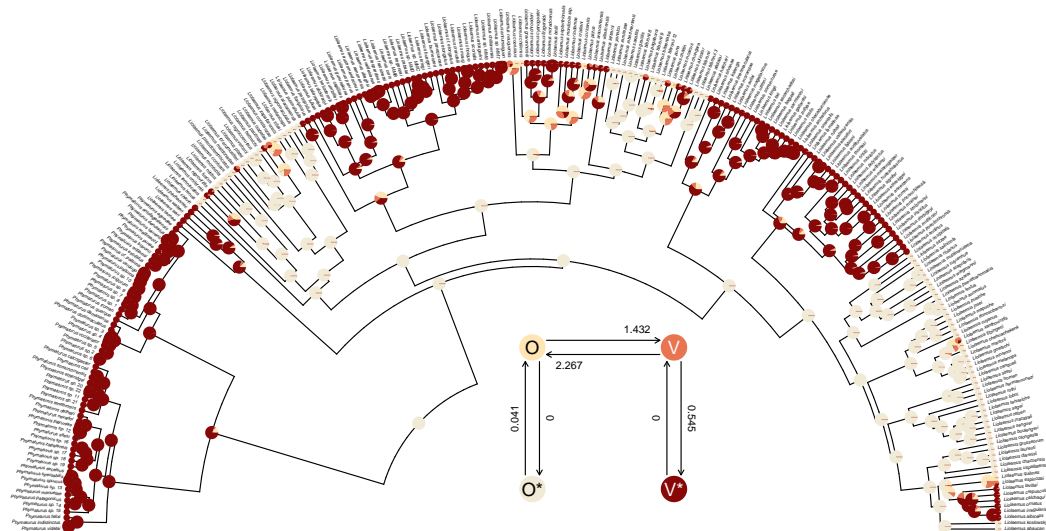


Figure 9. Marginal ancestral state reconstruction of parity mode (oviparity vs. viviparity) in liolaemid lizards under the hidden-rates model. Phylogeny and data based on Esquerré et al. (2019). Inset panel shows best-supported hidden-rates model. See main text for additional details.

```
619 ## 267 0.005267 0.993303 0.001430 0
620 ## 268 0.005649 0.992315 0.002037 0
621 ## 269 0.140376 0.820768 0.038856 0
622 ## ...
623 ##
624 ## Log-likelihood = -59.117373
```

625 Lastly, this marginal ancestral state reconstruction can easily be plotted on the tree using a *phytools*
626 `plot` method for the object class. Here, just for fun, I've also inset a visualization of our fitted umbral
627 hidden-rates model. We can see from this best-supported model that although the observed condition of
628 parity mode may not satisfy Dollo's Law (Lee and Shine 1998) in liolaemid lizards, under the umbral
629 model parity mode evolution *does* appear to have a hidden, absorbing (i.e., irreversible) viviparous
630 condition (Figure 9), from which oviparous reproductive mode can no longer re-evolve.

```
cols<-setNames(c("#FFE5B4", "#F0EAD6", "#E97451",
"#880808"), colnames(liolaemid.hrm_asr$ace))
plot(liolaemid.hrm_asr, legend=FALSE,
args.plotTree=list(type="arc", arc_height=0.5,
fsize=0.25, offset=5, xlim=c(-65, 65), ylim=c(0, 65)),
args.nodelabels=list(piecol=cols, cex=0.3),
args.tiplabels=list(cex=0.15))
pp<-plot(liolaemid.hrm, add=TRUE, xlim=c(-4, 2),
ylim=c(-1.3, 4.7), spacer=0.2, offset=0.1)
invisible(mapply(plotrix::draw.circle, x=pp$x, y=pp$y,
col=cols, MoreArgs=list(radius=strheight("0"),
border="transparent"))
text(pp$x, pp$y, pp$states, col=c("black", "black", "white",
"white"))
```

631 5 CONTINUOUS CHARACTERS

632 Numerous continuous trait methods exist in the *phytools* package. For example, *phytools* can be used
633 to measure phylogenetic signal (phylosig, Pagel 1999; Blomberg et al. 2003; Revell et al. 2008), it

can fit multi-rate Brownian evolution models (`brownie.lite`, `brownieREML`, `evol.rate.mcmc`, `multirateBM`, `ratebytree`, and `rateshift`, O'Meara et al. 2006; Revell et al. 2012, 2018; Revell 2021; Revell and Harmon 2022), it can perform phylogenetic canonical correlation and principal components analysis (`phyl.cca` and `phyl.pca`, Revell and Harrison 2008; Revell 2009), it can reconstruct ancestral states under multiple evolutionary models (`anc.Bayes`, `anc.ML`, `anc.trend`, and `fastAnc`, Schluter et al. 1997; Revell and Harmon 2022), it can use continuous trait data to place a fossil or missing lineage into a reconstructed tree (`locate.fossil` and `locate.yeti`, Felsenstein 2002; Revell et al. 2015), it can fit a multivariate Brownian model with multiple evolutionary correlations on the tree (`evol.vcv` and `evolvcv.lite`, Revell and Collar 2009; Revell et al. 2022), and it can perform various types of continuous character numerical simulation on phylogenies (e.g., `branching.diffusion`, `fastBM`, `sim.corrs`, `sim.rates`).

Here I'll start by illustrating the measurement of phylogenetic signal (`phylosig`), then I'll demonstrate Bayesian ancestral state estimation (`anc.Bayes`). I'll show how to fit a variable-correlation multivariate Brownian trait evolution model (`evolvcv.lite`), and, finally, I'll demonstrate a relatively new multi-rate trait evolution model that uses the estimation technique of penalized likelihood (`multirateBM`).

5.1 Phylogenetic signal

Perhaps the simplest phylogenetic comparative analysis that we could choose to undertake for a continuous trait data in R is the measurement of phylogenetic signal (Pagel 1999; Blomberg et al. 2003; Revell et al. 2008). Phylogenetic signal has been defined in a number of different ways, but could be considered to be the basic tendency of more closely related species to bear more similarity (one to another) than they do to more distant taxa (Revell et al. 2008). Apart from its definition, phylogenetic signal can likewise be *quantified* in various manners; however, undoubtedly the two most popular metrics are Blomberg et al.'s (2003) *K* statistic, and Pagel's (1999) λ . Conveniently, both of these can be calculated using the *phytools* package.

To get started in this undertaking, let's load some data from *phytools* consisting of a phylogenetic tree of eelopomorph eels and a data frame of phenotypic traits. Both tree and data were obtained from an article by Collar et al. (2014) and are now packaged with *phytools*.

```
data(eel.tree)
data(eel.data)
head(eel.data)
```

```
##              feed_mode Max_TL_cm
## Albula_vulpes    suction      104
## Anguilla_anguilla suction       50
## Anguilla_bicolor  suction      120
## Anguilla_japonica suction      150
## Anguilla_rostrata suction      152
## Ariosoma_anago    suction       60
```

Having loaded these data, we'll next extract one variable from our data array. Phylogenetic signal can be measured for any continuous trait, so we'll use maximum total length: here represented by the column of our data frame called "Max_TL_cm". As is often the case, we'll transform our data to a log scale. (There are multiple reasons log transformations are favored by comparative biologists working on interspecies data. One is that it makes a, say, 10% change equal, regardless of whether it occurs in an elephant or a mouse! See Revell and Harmon 2022 for more details.)

```
eel.lnTL <- setNames(log(eel.data$Max_TL_cm),
  rownames(eel.data))
```

Next, we'll compute a value of the *K* statistic of Blomberg et al. (2003) using the *phytools* function `phylosig`. `phylosig` calculates *K* by default (that is, without specifying an argument for `method`), but if I add the argument value `test=TRUE`, `phylosig` will also conduct a statistical test of the measured value of *K* by comparing it to a null distribution of *K* obtained by permuting our observed trait values randomly across the tips of the phylogeny.

```
eel.Blomberg_K<-phylosig(eel.tree,eel.lnTL,test=TRUE)
eel.Blomberg_K
```

```
##
## Phylogenetic signal K : 0.362879
## P-value (based on 1000 randomizations) : 0.036
```

K has an expected value of 1.0 under Brownian motion (Blomberg et al. 2003). The lower value that we observe here thus indicates less phylogenetic signal than expected under Brownian evolution; whereas a value higher than 1.0 would've indicated more. Our significance test shows us that this value of K , though numerically modest, is nonetheless significantly greater than we'd expect to find in data that were entirely random with respect to the tree!

In addition to Blomberg et al.'s K , *phytools* also can be used to estimate Pagel's (1999) λ statistic. λ measures phylogenetic signal as a scalar multiplier of the correlations of related taxa in our tree (Revell and Harmon 2022). That is to say, if λ has a value less than 1.0, this would indicate that related species in our phylogeny have a lower degree of "autocorrelation" than expected under Brownian evolution. In fact, a value of λ close to zero could be taken to indicate that related species are not phenotypically correlated at all!

We use Maximum Likelihood to find the value of λ that makes our observed data most probable. Since it's straightforward to compute a likelihood for any allowable value of λ , including $\lambda = 0$, we can very easily proceed to test a null hypothesis of no phylogenetic signal in our data by simply calculating a likelihood ratio in which we compare $\lambda = 0$ to our Maximum Likelihood estimate. Indeed, this is the test performed by *phytools* if `method="lambda"` and `test=TRUE`!

```
eel.Pagel_lambda<-phylosig(eel.tree,eel.lnTL,
  method="lambda",test=TRUE)
eel.Pagel_lambda
```

```
##
## Phylogenetic signal lambda : 0.673729
## logL(lambda) : -54.3016
## LR(lambda=0) : 5.18173
## P-value (based on LR test) : 0.0228256
```

This result tells us that we've found significant phylogenetic signal in our trait by both measures. Although K and λ tend to be correlated, it's entirely possible that we could've found significant K and non-significant λ , or vice versa. This is not a contradiction. The concept of phylogenetic signal is one of phenotypic similarity among related species – but K and λ measure this concept via two entirely different procedures!

Along with the simple calculation of phylogenetic signal, *phytools* also contains several methods to visualize our results. In particular, for Blomberg et al.'s K we can plot the permutation distribution of K alongside our observed measure. For Pagel's λ , we can plot the likelihood surface, our Maximum Likelihood solution, and the likelihood of $\lambda = 0$: the null hypothesis of our statistical tests. Both of these plots are illustrated in Figure 10 for our eel body length data.

```
par(mfrow=c(1,2),cex=0.9)
plot(eel.Blomberg_K,las=1,cex.axis=0.9)
mtext("a",adj=0,line=1)
plot(eel.Pagel_lambda,bty="n",las=1,cex.axis=0.9,
  xlim=c(0,1.1))
mtext("b",adj=0,line=1)
```

5.2 Bayesian ancestral state estimation

The *phytools* package contains several different functions for discrete and continuous character ancestral state estimation under multiple models. Earlier, we reviewed the method of stochastic character mapping

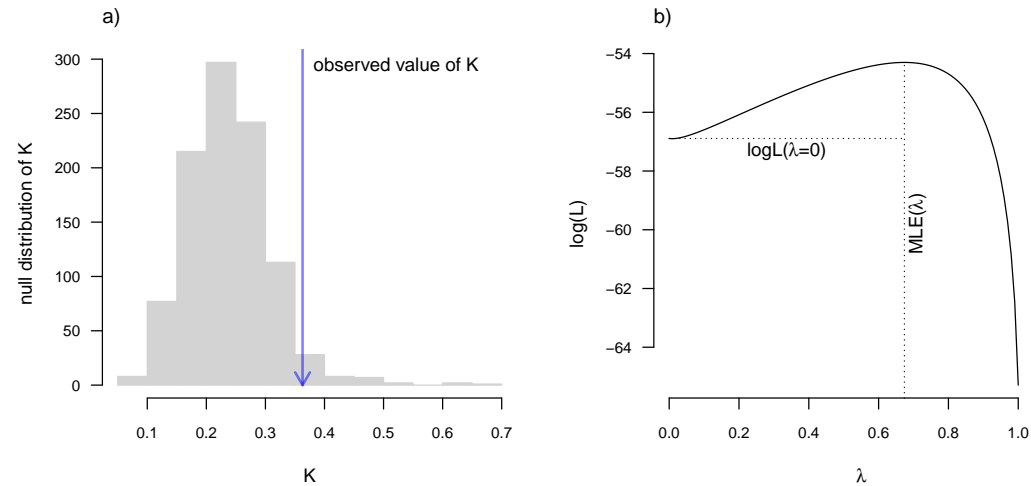


Figure 10. a) Blomberg et al. (2003) measured value of the K statistic for phylogenetic signal, compared to a null distribution of K obtained via randomization. b) Pagel's (1999) λ statistic for phylogenetic signal, also showing the likelihood surface. Data consist of maximum body length (on a log scale) from 61 species of eelomorph eels (Collar et al. 2014). See main text for additional details.

(Huelsenbeck et al. 2003) and marginal ancestral character estimation, both of which are important tools for ancestral state reconstruction of discretely-valued traits.

Among the variety of approaches for ancestral character estimation of continuous characters that are implemented in the *phytools* package is the function `anc.Bayes`. As its name suggests, `anc.Bayes` performs ancestral state estimation using Bayesian MCMC. Just as any proper Bayesian approach should, the implementation of this method allows us to include prior information about the states at internal nodes. Here, I'll illustrate the simplest type of analysis that we can undertake with the function in which I'll simply accept the default node priors and MCMC conditions. `anc.Bayes`, however, will be most useful when we intend to explicitly incorporate prior knowledge about internal nodes of the tree – based on, for instance, observations from the fossil record.

To demonstrate the method, I'll load a dataset (now packaged with *phytools*) that consists of a phylogeny and phenotypic trait information for a set of lizards from the family Cordylidae, originally published by Broeckhoven et al. (2016).

```
data(cordylid.tree)
data(cordylid.data)
head(cordylid.data)
```

```
##          pPC1      pPC2      pPC3
## C._aridus  0.59441 -0.40209  0.57109
## C._minor   0.65171 -0.32732  0.55692
## C._imkeae  0.19958 -0.08978  0.56671
## C._mclachlani 0.62065  0.03746  0.86721
## C._macropholis 0.44875 -0.75942  0.09737
## C._cordylus -0.07267  0.48294 -0.54394
```

Our trait data in this case are species scores for three different principal component (PC) axes from a phylogenetic principal components analysis undertaken using the *phytools* `phyl.pca` function (Revell 2009). Cordylid lizards are known for their body and tail armor, consisting of large, rectangular scales called osteoderms. Principal component 1 in Broeckhoven et al. (2016) separated the most lightly armored cordylids (large negative values), from those cordylids with the heaviest body armor (large positive values of PC 1). Why don't we extract this principal component from our data frame and rename it, as follows?


```
cordylid.armor.score<-setNames(cordylid.data$PC1,
rownames(cordylid.data))
```

743 With this named trait vector at the ready, we're prepared to undertake our Bayesian MCMC. As noted
744 above, we'll use the default conditions but update the number of generations that we want our MCMC to
745 run to `ngen=500000`. Depending on the size of our phylogenetic tree, we may want to run more (or
746 fewer) generations in a genuine empirical study.

```
cordylid.mcmc<-anc.Bayes(cordylid.tree,
cordylid.armor.score,ngen=500000)
```

```
747 ## List of 7
748 ## $ sig2 : num 0.713
749 ## $ a : num [1, 1] 0.000422
750 ## $ y : num [1:26] 0.000422 0.000422 0.000422 0.000422 ...
751 ## $ pr.mean: num [1:28] 1000 0 0 0 0 0 0 0 0 0 ...
752 ## $ pr.var : num [1:28] 1e+06 1e+03 1e+03 1e+03 1e+03 1e+03 ...
753 ## $ prop : num [1:28] 0.00713 0.00713 0.00713 0.00713 ...
754 ## $ sample : num 100
755
756 ## Starting MCMC...
757
758 ## Done MCMC.
```

759 We can see that the method starts by printing out a summary of the “control parameters” of the MCMC.
760 These include: initial values for the Brownian rate, σ^2 (`sig2`), the root state (`a`), and the internal node
761 values (`y`); information about our prior probability distributions (`pr.mean` and `pr.var`); the variances
762 of the proposal distributions on each variable in the model (`prop`); and, finally, the interval that we'll use
763 to sample from our posterior distribution during the MCMC (`sample`). All of these parameters can be
764 adjusted by the *phytools* user.

765 The object class that results from this function call (`"anc.Bayes"`) has a `summary` method in
766 *phytools* that prints the mean from the posterior distribution, automatically excluding the first 20% of
767 our samples as burn-in (though we can adjust this percentage if we'd like). Though a thorough review of
768 Bayesian MCMC is beyond the scope of this article, burn-in refers to the number of generations required
769 for our MCMC to convergence on the posterior probability distribution, and will depend on numerous
770 factors including (but not limited to) our starting values, the parameter complexity of our model, and
771 the proposal distribution. (See Roy 2020 for a recent review of burn-in, convergence diagnostics, and
772 related topics.) Convergence can be diagnosed quantitatively via multiple methods, including using the R
773 package *coda* (Plummer et al. 2006). In addition to printing our results to screen, `summary` also passes
774 the estimates (normally invisibly, but we can save them to a new variable in our workspace as we've done
775 here) back to the user.

```
cordylid.ace<-summary(cordylid.mcmc)
```

```
776 ##
777 ## Object of class "anc.Bayes" consisting of a posterior
778 ## sample from a Bayesian ancestral state analysis:
779 ##
780 ## Mean ancestral states from posterior distribution:
781 ##      29      30      31      32      33      34
782 ## 0.059277 -0.099027 -0.106452 0.057220 0.153671 0.201722
783 ##      35      36      37      38      39      40
784 ## 0.225081 0.297659 0.392992 0.493316 0.015503 -0.006053
785 ##      41      42      43      44      45      46
786 ## 0.435309 0.392526 0.300532 0.210391 -1.505181 -1.857682
```

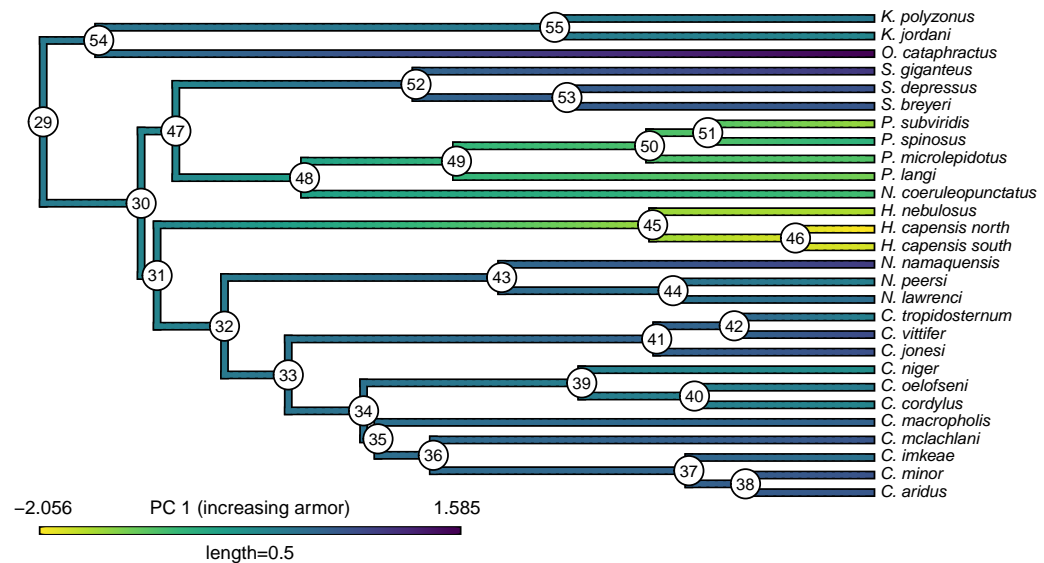


Figure 11. Reconstructed ancestral values from Bayesian MCMC projected onto the nodes and edges of the tree. Numerical values at internal nodes are node indices from our input phylogeny. Data consist of PC 1 from a phylogenetic principal components analysis of cordylid morphological traits, and separate highly armored (high values) from lightly armored (low values) lizards (Broeckhoven et al. 2016). See main text for more details.

```

787 ##          47          48          49          50          51          52
788 ## -0.136014 -0.520322 -0.829181 -0.985510 -1.040208  0.385293
789 ##          53          54          55
790 ##  0.511646  0.159943  0.028358
791 ##
792 ## Based on a burn-in of 1e+05 generations.

```

Now that we've obtained our estimated Bayesian ancestral states for internal nodes, it's a straightforward task to visualize them on the branches and nodes of the tree. For this undertaking we'll use the popular *phytools* plotting function `contMap` (Revell 2013). By default, `contMap` uses Maximum Likelihood to compute ancestral states at all of the internal nodes of the tree – but it can also be supplied with user-specified values. Since we want to use our Bayesian estimates from `anc.Bayes`, that's what we'll do here.

```

cordylid.contMap<-contMap(cordylid.tree,
  cordylid.armor.score,anc.states=cordylid.ace,
  plot=FALSE)
cordylid.contMap<-setMap(cordylid.contMap,
  viridisLite::viridis(n=10,direction=-1))
plot(cordylid.contMap,ftype="i",fsize=c(0.6,0.7),
  leg.txt="PC 1 (increasing armor)",lwd=3)
nodeLabels(frame="circle",bg="white",cex=0.6)

```

For fun, compare Figure 11 to Figure 2 of Broeckhoven et al. in which estimated ancestral state values were assigned to each branch using a similar color gradient!

In addition to this simple analysis, we can (naturally) extract and plot posterior probability densities from any of our internal nodes of the tree. To see this, let's focus on the node labeled "49" in Figure 11 and do exactly that. Node 49 corresponds to the common ancestor of the *Pseudocordylus* clade. The *Pseudocordylus* are among the most lightly all cordylid lizards in this analysis, so we'd expect our posterior distribution for this node to be centered on a relatively low value of our armor score.

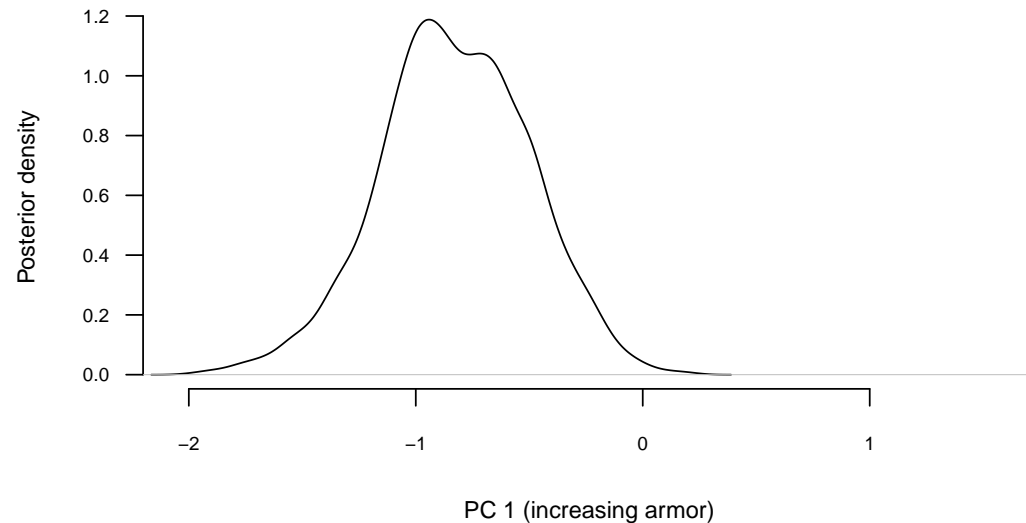


Figure 12. Posterior probability density at node 49 of Figure 10 from Bayesian MCMC ancestral state reconstruction of PC 1 from a morphological analysis on a phylogenetic tree of cordylid lizards. Node 49 corresponds to the common ancestor of the *Pseudocordylus*: a relatively lightly armored cordylid clade. See main text for more details.

```
cordylid.node49<-density(cordylid.mcmc,what=49)
cordylid.node49
```

```
806 ##
807 ## Call:
808 ## density.anc.Bayes(x = cordylid.mcmc, what = 49)
809 ##
810 ## Data: node 49 (4001 obs.); Bandwidth 'bw' = 0.05679
811 ##
812 ##      x              y
813 ##  Min.   : -2.1658   Min.   : 0.000023
814 ## 1st Qu.: -1.5270   1st Qu.: 0.022415
815 ## Median : -0.8883   Median : 0.187932
816 ## Mean   : -0.8883   Mean   : 0.391002
817 ## 3rd Qu.: -0.2495   3rd Qu.: 0.784591
818 ## Max.    :  0.3893   Max.    : 1.187968
```

```
par(mar=c(5.1,4.1,1.1,2.1))
plot(cordylid.node49,las=1,bty="n",main="",cex.lab=0.8,
      cex.axis=0.7,xlab="PC 1 (increasing armor)",
      ylab="Posterior density",
      xlim=range(cordylid.armor.score))
```

819 Figure 12 shows our estimate of the posterior probability distribution of the ancestral node 49 state,
820 and should be centered precisely on the value we projected onto the tree of Figure 11!

821 As given here, Bayesian MCMC ancestral state reconstruction will yield (in nearly all circumstances)
822 point estimates that are highly similar to the values that we might have obtained using Maximum
823 Likelihood. Nonetheless, Bayesian inference provides the additional benefit of supplying a natural
824 framework for incorporating prior information about the states at one or various internal nodes in the
825 tree (by adjusting `pr.mean`, `pr.var`, or both: see above), as well as for measuring the substantial

uncertainty that can be associated with ancestral trait estimates (in particular, by providing not just confidence intervals around each node, but sets of ancestral values across *all* nodes of the tree that have been sampled in proportion to their posterior probability under the model).

5.3 Multivariate trait evolution

Along with the various univariate methods we've seen so far, *phytools* also contains a handful of different multivariate trait evolution models, designed for both continuous and discrete characters.

One of these is an interesting model (described in Revell and Collar 2009; Revell et al. 2022) in which the rates and evolutionary correlations between traits are allowed to vary as a function of a set of mapped regimes on the tree. (Similar to O'Meara et al. 2006, but for more than one trait at a time.) The underlying motivation of this method is to test hypotheses about phylogenetic heterogeneity in the evolutionary relationship (i.e., correlation) between different traits on our phylogeny. This approach is also used to study quantitative trait modularity and integration during macroevolution (e.g., Damian-Serrano et al. 2021).

Note that closely related analyses have been implemented in the R packages *mvMORPH* by Clavel et al. (2015), and *ratematrix* by Caetano and Harmon (2017). The packages *mvSLOUCH* (Bartoszek et al. 2012), *PhylogeneticEM* (Bastide et al. 2018), and *PCMFIt* (Mitov et al. 2019) also feature phylogenetic multivariate quantitative trait analysis methods.

To illustrate our approach, however, I'll use a phylogenetic tree and dataset of tropidurid lizard species from Revell et al. (2022).

```
data(tropidurid.tree)
data(tropidurid.data)
```

In this case, our phylogeny is already a tree with mapped regimes. We can see this by merely printing the model object that we loaded. (In an empirical study we might imagine using a set of such trees sampled in proportion to their probabilities using stochastic mapping – and then averaging the result. E.g., see Revell et al. 2022.)

```
print(tropidurid.tree, printlen=2)
```

```
##
## Phylogenetic tree with 76 tips and 75 internal nodes.
##
## Tip labels:
## Leiocephalus_raviceps, Leiocephalus_carinatus, ...
##
## The tree includes a mapped, 2-state discrete character
## with states:
## n_rock, rock
##
## Rooted; includes branch lengths.
```

This tells us that our phylogenetic tree contains 76 taxa and a mapped regime with two states: "n_rock" (non-rock dwelling) and "rock" (rock-dwelling). Since *phytools* permits mapped regimes to have arbitrarily lengthy names, let's rename these two regime levels in a more informative way. To do so, I'll use the *phytools* function `mergeMappedStates`. `mergeMappedStates`, as readers can probably guess, is designed to merge the mappings of two or more traits into one – but can also be employed to simply substitute one mapping name for another!

```
tropidurid.tree<-mergeMappedStates(tropidurid.tree,
  "n_rock", "non-rock dwelling")
tropidurid.tree<-mergeMappedStates(tropidurid.tree,
  "rock", "rock-dwelling")
```

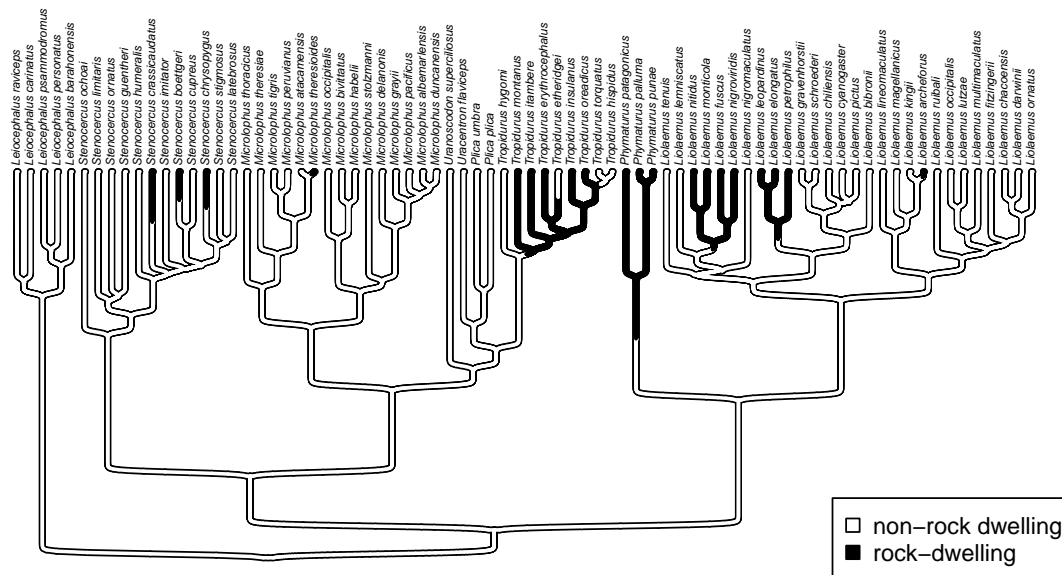


Figure 13. Phylogenetic tree of rock- and non-rock dwelling tropidurid lizard species from Revell et al. (2022). Mapped colors correspond to a hypothesis of the history of habitat use across the clade. See main text for more details.

866 Let's plot this updated tree. To do so, I'm going to use the recent *phytools* function
867 *sigmoidPhylogram* that will plot our tree using curved ("sigmoidal") linking lines. (*phytools*
868 contains lots of cool tree plotting functions like this one!)

```
cols<-setNames(c("white","black"),c("non-rock dwelling",
  "rock-dwelling"))
sigmoidPhylogram(tropidurid.tree,direction="upwards",
  outline=TRUE,colors=cols,direction="upwards",
  outline=TRUE,lwd=2,fsz=0.4,ftype="i",offset=1)
legend("bottomright",c("non-rock dwelling",
  "rock-dwelling"),pch=22,pt.bg=cols,cex=0.8,
  pt.cex=1.2)
```

869 Our quantitative phenotypic trait data in *tropidurid.data* consist of a single measure of overall
870 body size (as trait 1, "newsize"), and a second metric trait measuring dorsoventral depth (vs. flattening,
871 "body_height").

```
head(tropidurid.data)
```

```
##          newsize body_height
## Leiocephalus_raviceps  2.358317  0.05768818
## Leiocephalus_carinatus  2.931721  0.30216220
## Leiocephalus_psammmodromus  2.700397  0.19667083
## Leiocephalus_personatus  2.535315  0.32216983
## Leiocephalus_barahonensis  2.473666  0.30266917
## Stenocercus_ochoai  2.549010  0.29067644
```

879 Our hypothesis of multivariate trait evolution in this clade is that these two traits (size and body depth)
880 should generally scale together in non-rock dwelling lizard species: bigger lizards also tend to have
881 larger body depths. We hypothesize, however, that this general relationship may become decoupled in
882 rock-dwelling lineages where the force of selection is predicted to favor increased flattening, relative to

883 their non-rock dwelling kin. (There are biomechanical and behavioral reasons to suspect this could be so.
884 For more information, see Revell et al. 2007; Revell et al. 2022.)

885 To test this hypothesis, we'll use the *phytools* function `evolvcv.lite` which fits a heirarchical
886 set of models for the evolutionary rates (of each character) and evolutionary correlations (between them,
887 Revell and Collar 2009; Revell et al. 2022). Following Revell and Collar (2009), these models are: (1)
888 a model with common rates and correlations between the two discrete traits; (2) a model with different
889 rates of evolution depending on our mapped state, but a common correlation; (3) a model with common
890 rates, but a different evolutionary correlation, depending on the mapped discrete character; and, finally,
891 (4) a model of different rates and correlations between the two discrete mapped character states.

```
tropidurid.fits<-evolvcv.lite(tropidurid.tree,  
tropidurid.data)
```

```
892 ## Fitting model 1: common rates, common correlation...  
893 ## Best log(L) from model 1: 52.3056.  
894 ## Fitting model 2: different rates, common correlation...  
895 ## Best log(L) from model 2: 54.3968.  
896 ## Fitting model 3: common rates, different correlation...  
897 ## Best log(L) from model 3: 55.1105.  
898 ## Fitting model 4: no common structure...  
899 ## Best log(L) from model 4: 56.2877.
```

900 Having fit each of four models (in this case: `evolvcv.lite` actually includes several additional
901 models that we won't review here, see Revell et al. 2022 for more details), we can most easily compare
902 all of the models in our set using a generic `anova` function call as follows.

```
anova(tropidurid.fits)
```

```
903 ##           log(L) d.f.         AIC      weight  
904 ## model 1 52.30560    5 -94.61119 0.09221085  
905 ## model 2 54.39681    7 -94.79362 0.10101737  
906 ## model 3 55.11048    6 -98.22096 0.56057434  
907 ## model 4 56.28765    8 -96.57530 0.24619744
```

908 This comparison shows us that our third model ("model 3": remember, with common rates but
909 different evolutionary correlation between rock and non-rock dwelling species) is the best-supported
910 explanation of our data in this set, with the lowest AIC score and highest model weight. We can print out
911 a summary of our set of four models to review the estimated parameter values of each.

```
tropidurid.fits
```

```
912 ## Model 1: common rates, common correlation  
913 ## R[1,1] R[1,2] R[2,2] k log(L) AIC  
914 ## fitted 0.2224 0.0154 0.0589 5 52.3056 -94.6112  
915 ##  
916 ## (R thinks it has found the ML solution for model 1.)  
917 ##  
918 ## Model 2: different rates, common correlation  
919 ## R[1,1] R[1,2] R[2,2] k log(L) AIC  
920 ## non-rock dwelling 0.2025 0.0187 0.0456 7 54.3968 -94.7936  
921 ## rock-dwelling 0.3043 0.0382 0.1263  
922 ##  
923 ## (R thinks it has found the ML solution for model 2.)  
924 ##  
925 ## Model 3: common rates, different correlation  
926 ## R[1,1] R[1,2] R[2,2] k log(L) AIC
```

```

927 ## non-rock dwelling      0.2256  0.0394  0.0588  6   55.1105 -98.221
928 ## rock-dwelling         0.2256 -0.0354  0.0588
929 ##
930 ## (R thinks it has found the ML solution for model 3.)
931 ##
932 ## Model 4: no common structure
933 ## R[1,1] R[1,2] R[2,2] k log(L) AIC
934 ## non-rock dwelling      0.2108  0.0325  0.0485  8   56.2877 -96.5753
935 ## rock-dwelling          0.2794 -0.0564  0.101
936 ##
937 ## (R thinks it has found the ML solution for model 4.)

```

Here we see that model 3 is one in which the evolutionary covariance between overall body size and dorsoventral flattening is *negative* among rock-dwelling lineages – compared to the positive evolutionary covariance in non-rock species and across all other models. Just as we’d predicted, size and body depth are evolutionarily decoupled in rock-dwelling specialists!

5.4 Variable rate Brownian motion

Lastly, I recently added a function to *phytools* that permits us to fit a variable-rate Brownian evolution model using penalized likelihood (Revell 2021). Related methods have been implemented both outside (e.g., Venditti et al. 2011) and inside (e.g., Uyeda and Harmon 2014; Martin et al. 2022) R.

In our model, we’ll assume that the phenotypic trait evolves via a standard Brownian motion process – but that the rate of evolution (σ^2) itself also changes through time and among the clades of our tree via a process of *geometric* Brownian motion. (That is, Brownian motion on a log scale.) As one might expect for a penalized likelihood method, when we go ahead and fit this model to data, the degree to which the evolutionary rate is permitted to vary from edge to edge in the tree is controlled by our λ penalty or “smoothing” coefficient (Revell 2021).

Although a relatively new addition to the *phytools* package, this method has already been used to, for example, investigate rate heterogeneity differences in body size evolution between cetaceans and plesiosaurs (Sander et al. 2021), and to measure rate variation in the evolution of the mechanical properties of woody plant tissue (Higham et al. 2022). Here, I’ll apply it to the analysis of skull size evolution in a phylogenetic tree of primates. My data for this example (now packaged with *phytools*) come from a book chapter authored by Kirk and Kay (2004).

```

data(primate.tree)
data(primate.data)

```

Our data frame, `primate.data`, contains a number of different variables. Let’s pull out just one of these, `Skull.length`, and (as we do) convert it to a logarithmic scale.

```

primate.lnSkull<-setNames(
  log(primate.data$Skull.length),
  rownames(primate.data))
head(primate.lnSkull)

```

```

960 ## Allenopithecus_nigroviridis      Alouatta_palliata
961 ##                               4.590057                4.698661
962 ##           Alouatta_seneculus      Aotus_trivirgatus
963 ##                               4.682131                4.102643
964 ##           Arctocebus_aureus      Arctocebus_calabarensis
965 ##                               3.901973                3.985273

```

With just this input data vector and our tree, we’re already ready to run our penalized likelihood analysis. As I mentioned earlier, however, penalized likelihood requires the user to specify a smoothing parameter – normally denominated λ . λ determines the weight that’s assigned to the penalty term of the fitted model, in our case a measure of how much (or how little) the evolutionary rate evolves from

edge to edge in the phylogeny (Revell 2021). A large value of λ will more stringently penalize high rate variation between edges and thus cause us to fit a model with relatively low rate heterogeneity across the tree. Smaller values of λ , on the other hand, should have the converse effect.

A number of approaches, such as cross-validation (e.g., Efron and Gong 1983), have been suggested to help us identify suitable values of λ in penalized likelihood for our data and question – however, I’d *minimally* recommend testing multiple values of λ and comparing the results! Let’s do exactly that for our analysis of primate skull length: first using $\lambda = 1.0$, and then swapping it for a much smaller $\lambda = 0.1$ and much larger $\lambda = 10$. This will allow us to pretty quickly see how these different values of our smoothing parameter affect our findings, and thus how sensitive any inference we draw might be to the specific value of λ we assigned!

Before continuing, however, we’ll try to get a better sense of our data by creating a simple projection of our phenotypic trait (log skull length) onto the tree. Visual inspection may help give us a preliminary sense of where in our tree our penalized likelihood method could end up showing the rate of primate skull length evolution to vary the most – and the least. In this case, I’ll use two different plotting methods.

First, I’ll use the *phytools* function `edge.widthMap` which sizes the thickness of our plotted branches in proportion to the observed or reconstructed trait values. (This is one of my favorite *phytools* functions, but, compared to the `contMap` method we saw earlier, so far as I can tell it’s been used very little in published literature!) We can see the result in Figure 14a. In addition to this visualization, I’ll also undertake a simple projection of our phylogeny into the trait space. This is done using a very popular *phytools* plotting method called `phenogram` (Evans et al. 2009; Revell 2013; Revell 2014b). In the typical style of this kind of plot, our phylogeny is graphed in a space defined by time since the root of the tree (on our horizontal axis), and the observed or reconstructed values of our phenotypic trait (on the vertical, Revell 2013). The result of this projection is shown in Figure 14b.

```
par(mfrow=c(1,2))
primate.widthMap<-edge.widthMap(primate.tree,
  primate.lnSkull)
plot(primate.widthMap,color=palette()[4],
  legend="log(skull length)",border=TRUE,fsz=0.4,
  mar=c(4.1,1.1,2.1,0.1))
mtext("a",adj=0,line=0,cex=1.4)
phenogram(primate.tree,primate.lnSkull,fsz=0.4,
  ftype="i",spread.cost=c(1,0),mar=c(4.1,4.1,2.1,0.1),
  quiet=TRUE,las=1,cex.axis=0.8,
  ylab="log(skull length)")
mtext("b",adj=0,line=0,cex=1.4)
```

The function we’ll use to fit our rate-variable model, `multirateBM`, performs a computationally intensive optimization. Setting the optional argument `parallel=TRUE` will help distribute this burden across multiple processors of our computer, if possible. Let’s start our analysis using a smoothing parameter, λ , equal to $\lambda = 1.0$.

```
primate.mBM.1<-multirateBM(primate.tree,
  primate.lnSkull,lambda=1,parallel=TRUE)
```

```
## Beginning optimization....
## Using socket cluster with 16 nodes on host 'localhost'.
## Optimization iteration 1. Using "L-BFGS-B" (parallel)
## optimization method.
## Best (penalized) log-likelihood so far: -267.108
## Done optimization.
```

Now we can do the same with $\lambda = 0.1$ and 10 . Readers should take special care to note that the specific values of the penalized log likelihoods are not comparable between analyses with different values of the penalty coefficient, λ ! This time I’ll turn off printing by updating the optional argument to `quiet=TRUE`.

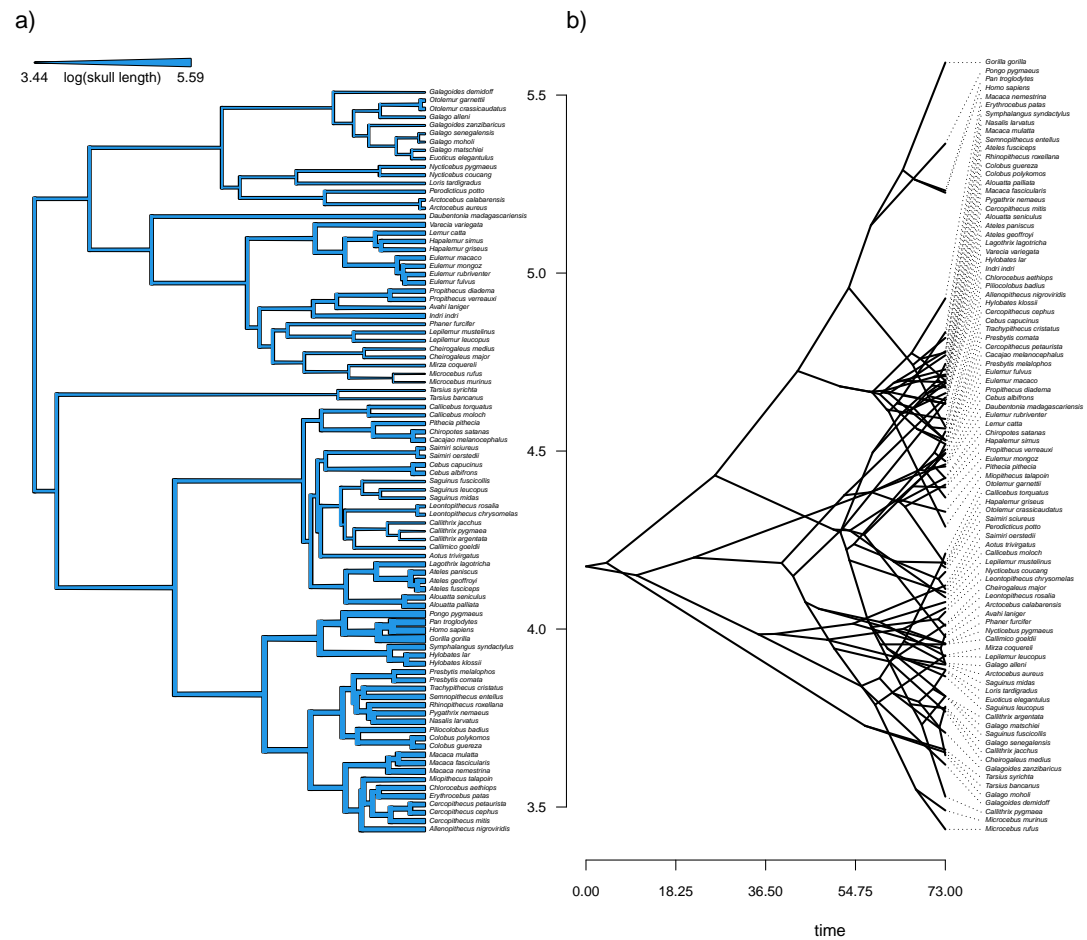


Figure 14. a) Primate skull lengths (on a log scale) projected onto the edges and nodes of the phylogeny. The width of each edge of the tree is proportional to the observed or reconstructed value of the trait. See main text for more details. b) A projection of the phylogeny of a) into a space defined by time since the root (on the horizontal axis) and log skull length. Phylogeny and data are derived from Kirk and Kay (2004). See main text for more details.

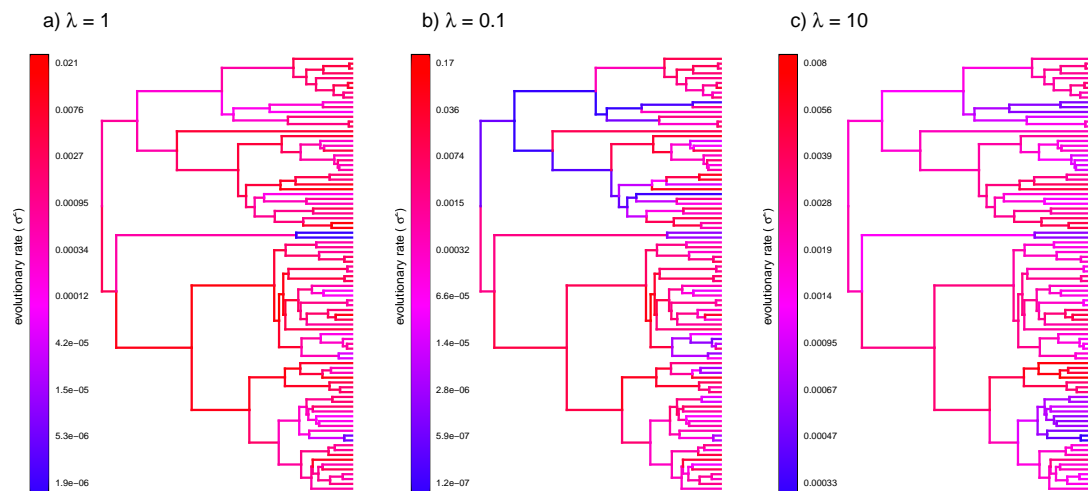


Figure 15. Estimated rates of log(skull length) evolution in primates under a variable-rate Brownian evolution model for different values of the smoothing parameter, λ . Increasing values of λ should correspond to less variation in the rate of evolution across the tree. Phylogeny and data are based on Kirk and Kay (2004). See main text for additional details.

```
primate.mBM_0.1<-multirateBM(primate.tree,
  primate.lnSkull,lambd=0.1,parallel=TRUE,quiet=TRUE)
primate.mBM_10<-multirateBM(primate.tree,
  primate.lnSkull,lambd=10,parallel=TRUE,quiet=TRUE)
```

Finally, let's visualize the differences and similarities between each of our three fitted models.

```
par(mfrow=c(1,3))
plot(primate.mBM_1,ftype="off",lwd=2,
  mar=c(0.1,0.1,2.1,0.1))
mtext(expression(paste("a)",lambda," = 1")),adj=0.1,
  line=0.5,cex=1.1)
plot(primate.mBM_0.1,ftype="off",lwd=2,
  mar=c(0.1,1.1,2.1,0.1))
mtext(expression(paste("b)",lambda," = 0.1")),adj=0.1,
  line=0.5,cex=1.1)
plot(primate.mBM_10,ftype="off",lwd=2,
  mar=c(0.1,1.1,2.1,0.1))
mtext(expression(paste("c)",lambda," = 10")),adj=0.1,
  line=0.5,cex=1.1)
```

We can see from the plot of Figure 15 that even though the specific range of rate variation depends strongly on our specified values of λ , the pattern from clade to clade on the tree is relatively robust. This should give us some measure of confidence that the our inferred rate heterogeneity may be a product of real variability in the evolutionary rate for our character on the phylogeny!

6 DIVERSIFICATION

In addition to the methods that we've seen so far, *phytools* also contains a handful of different techniques for investigating diversification on reconstructed phylogenies. Diversification has never been the primary focus of the *phytools* R package (to that end, I'd recommend the powerful *diversitree* package, FitzJohn 2012), but these methods are popular, and the *phytools* implementations can be relatively easy to use. Various additional R package include interesting diversification models and methods, including *hisse*

(Beaulieu and O’Meara 2016), *RPANDA* (Morlon et al. 2016), *TreeSim* (Stadler 2019), *DDD* (Etienne and Haegeman 2023), and others.

phytools contains methods to compute and visualize the accumulation of lineages through time, including with extinction (`ltt`), to calculate and test the γ statistic (`gammatest`, `mccr`, Pybus and Harvey 2000), to fit pure-birth and birth-death models, including with random missing taxa (`fit.yule` and `fit.bd`, Nee et al. 1994; Stadler 2013), to compare diversification rates between trees (`ratebytree`, Revell 2018), and to simulate stochastic trees under various conditions (`pbtrees`).

6.1 Lineage through time plots

One of the most rudimentary phylogenetic methods for studying diversification is to simply graph the accumulation of new lineages in our reconstructed phylogeny over time since the global root of the tree. This visualization method is called a lineage-through-time plot. A great appeal of this visualization is that if we graph the number of lineages through time in a fully-sampled pure-birth (that is, constant-rate speciation, but no extinction) phylogenetic tree, the accumulation curve should be exponential – or exactly linear on a semi-logarithmic scale. This means that the lineage-through-time plot gives us a handy tool that we can use to compare the real lineage accumulation in our reconstructed tree to this simple, neutral expectation (Pybus and Harvey 2000; Revell and Harmon 2022).

To see how the number of lineages through time are calculated and graphed using *phytools*, let’s load a phylogenetic tree of snakes from the venomous family Elapidae. This phylogeny is now packaged with *phytools* but derives from a study by Lee et al. (2016).

```
data(elapidae.tree)
print(elapidae.tree, printlen=2)

##
## Phylogenetic tree with 175 tips and 174 internal nodes.
##
## Tip labels:
## Calliophis_bivirgata, Calliophis_melanurus, ...
##
## Rooted; includes branch lengths.
```

We’re going to create our lineage-through-time graph with *phytools* over two steps. First, we’ll use the *phytools* function `ltt` to compute an object of class "`ltt`" containing our tree and a count of the number of lineages through time from the root of the tree to the tips.

```
elapidae.ltt <- ltt(elapidae.tree, plot=FALSE)
elapidae.ltt

## Object of class "ltt" containing:
##
## (1) A phylogenetic tree with 175 tips and 174 internal
## nodes.
##
## (2) Vectors containing the number of lineages (ltt) and
## branching times (times) on the tree.
##
## (3) A value for Pybus & Harvey’s "gamma" statistic of
## gamma = -3.3244, p-value = 9e-04.
```

From the print-out we see that in addition to the tree and the lineages through time, our object also contains a value of (and a P-value for) Pybus and Harvey’s (2000) γ statistic. γ is a numerical value used to describe the general shape of the lineage through time curve. If the curve is straight (on a semi-log scale), then γ should have a value close to zero. This is what we expect under a pure-birth (speciation only) diversification process. On the other hand, significantly positive or significantly negative γ mean that the lineage through time graph curves upward or downward towards the present day (Pybus and Harvey

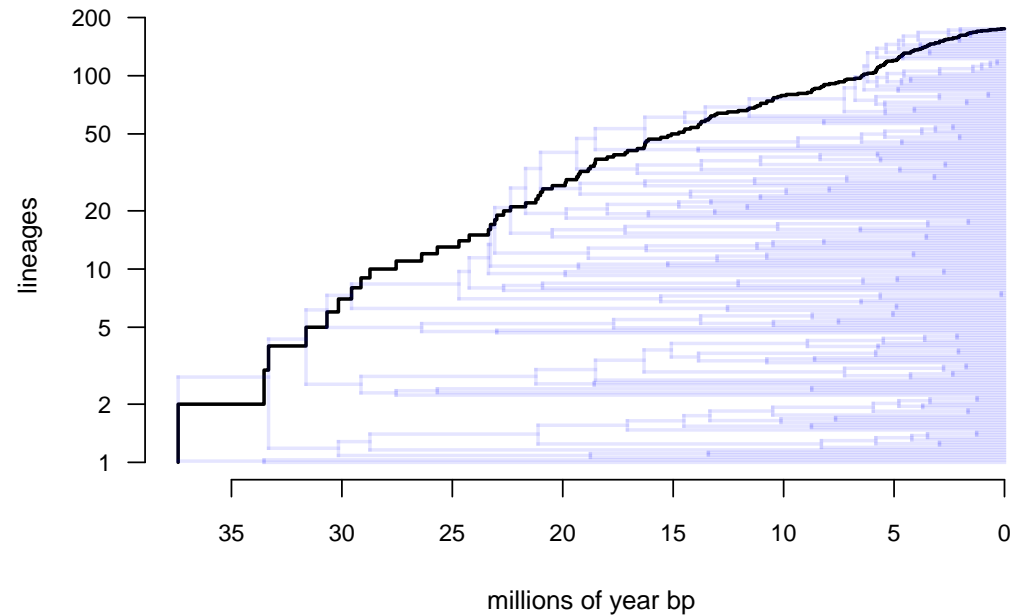


Figure 16. Lineage through time plot for phylogeny of snakes from the family Elapidae (Lee et al. 2016). See main text for more details.

2000). Significant positive or negative curvature of the lineage-through-time plot might mean that the rate of diversification has changed over time, but it could also be due to past extinction or incomplete taxon sampling (Revell and Harmon 2022). Note that since the pull of the present (Nee et al. 1992) means that our lineage through time plot is expected to curve upwards towards the present day for any non-zero rate of extinction, some have argued that γ should only be interpreted when *negative*. (I.e., that statistical tests of γ are properly one-tailed.) I don't subscribe to that view, inasmuch as I see γ as a phenomenological measure of lineage accumulation in our reconstructed tree whose positive or negative deviation from the statistic's expected value under pure-birth could have multiple underlying causes. At first look, the value of γ from our elapid snake phylogeny would seem to be highly significantly *negative*.

To proceed and graph our object created in the previous step, we merely need to execute a generic `plot` method function call as follows. A simple `plot` call would have done the trick; however, in this case I decided to first leave off the axes of my plot, and then re-plot them so that I could make our horizontal (x) axis run *backwards* in time (i.e., right to left) from the present day into the past. I've also super-imposed the phylogeny itself on our plot so that we can more easily visualization the relationship between the structure of our phylogenetic tree and the accumulation of lineages over time.

```
par(mar=c(5.1, 4.1, 1.1, 2.1))
plot(elapidae.ltt, show.tree=TRUE, lwd=2,
     log.lineages=FALSE, log="y", bty="n", cex.lab=0.9,
     transparency=0.1, axes=FALSE,
     xlab="millions of year bp")
h<-max(nodeHeights(elapidae.tree))
axis(1, at=h-seq(0, 35, by=5), labels=seq(0, 35, by=5), las=1,
     cex.axis=0.8)
axis(2, las=1, cex.axis=0.8)
```

In general, accounting for incomplete taxon sampling in the measurement of the γ statistic is important because missing taxa will tend to pull our lineage-through-time curve downwards as we approach the tips of the tree – in other words, towards more negative values of γ , just like the value that we see for our lineage through time plot of Figure 16.

1081 Fortunately, there's a simple way to address this bias. If we know the *true* species richness of our
1082 clade of interest, we can simply simulate trees that match this richness under pure-birth, randomly prune
1083 taxa to the level of "missingness" in our reconstructed tree, and then use the distribution of γ values across
1084 this set of simulated (and then randomly pruned) trees as our null distribution for hypothesis testing! This
1085 exact procedure is called the "Monte Carlo constant rates" (MCCR, Pybus and Harvey 2000) test and is
1086 implemented in the *phytools* function `mccr`.

1087 Of course, since the MCCR test accounts for randomly missing taxa from our tree, we must know or
1088 hypothesize a true species richness of our clade. In this instance, we're not too preoccupied about the
1089 precise value for Elapidae, but Lee et al. (2016) purported that their phylogeny included approximately
1090 50% of known elapids at the time. Even though it's likely that elapid diversity has changed a bit in the
1091 intervening years, for illustrative purposes only, let's just go with this 50% figure! In both `mccr` and the
1092 birth-death model-fitting function we'll use later, sampling fraction is specified via the argument `rho` (for
1093 the Greek letter ρ).

```
elapidae.mccr<-mccr(elapidae.ltt,rho=0.5,nsim=1000)
elapidae.mccr
```

```
1094 ## Object of class "mccr" consisting of:
1095 ##
1096 ## (1) A value for Pybus & Harvey's "gamma" statistic of
1097 ##      gamma = -3.3244.
1098 ##
1099 ## (2) A two-tailed p-value from the MCCR test of 0.446.
1100 ##
1101 ## (3) A simulated null-distribution of gamma from 1000
1102 ##      simulations.
```

1103 This tells us that, having accounted for missing taxa, our observed value of γ (previously highly
1104 significantly negative) becomes indistinguishable from what we'd expect under pure-birth. We can plot
1105 our results to see what I mean.

```
par(mar=c(5.1,4.1,0.6,2.1))
plot(elapidae.mccr,las=1,cex.lab=0.8,cex.axis=0.7,
     main="")
```

1106 Figure 17 shows that the measured value of γ by the MCCR test is no longer significant, demonstrating
1107 the vital importance of accounting for incomplete taxon sampling in this (and other) diversification
1108 analyses using phylogenies.

1109 6.2 Modeling speciation and extinction

1110 In addition to these analysis, *phytools* can also fit simple speciation and extinction models following Nee
1111 et al. (1994; Stadler 2013; Harmon 2019). This is done primarily using the function `fit.bd`, which also
1112 allows us to take into account an incomplete taxonomic sampling fraction (Stadler 2013).

1113 Just as with γ , incomplete sampling has the potential to substantially distort our estimated rates of
1114 speciation (normally given as λ – a different λ from before!) and extinction (μ). In this case, ignoring
1115 (or underestimating) the missing lineages in our tree will tend to cause us to underestimate the rate of
1116 extinction, as nearly all of the information we have about extinction comes from the most recent parts of
1117 our phylogeny! (See Stadler 2013; Harmon 2019; Revell and Harmon 2022 for more details.)

1118 Fitting a birth-death model using *phytools* is very easy. For this example, we'll use phylogenetic
1119 tree of lizards from the diverse South American family Liolaemidae. Just as in the other examples this
1120 phylogeny is packaged with *phytools*, but was originally published by Esquerré et al. (2019). (This is
1121 the same phylogeny that was used to study the evolution of parity mode evolution under the hidden rates
1122 model in an earlier section.)

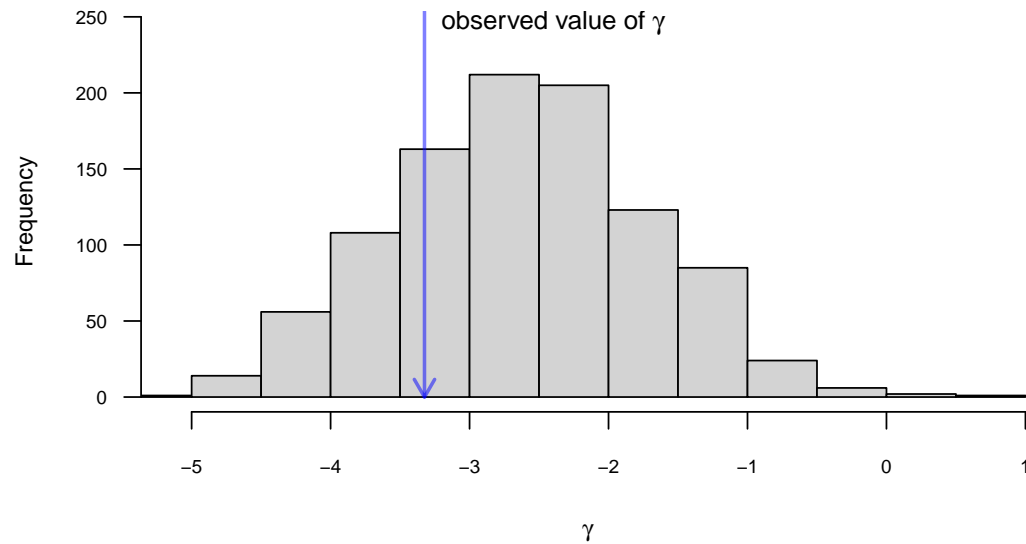


Figure 17. Distribution of simulated values of γ for the MCCR test, and observed value for the lineage through time curve of the phylogeny of elapid snakes given in Figure 15. Phylogenetic tree based on Lee et al. (2016). See main text for more details.

```
data(liolaemid.tree)
print(liolaemid.tree, printlen=2)
```

```
1123 ##
1124 ## Phylogenetic tree with 257 tips and 256 internal nodes.
1125 ##
1126 ## Tip labels:
1127 ##   Liolaemus_abaucan, Liolaemus_koslowskyi, ...
1128 ##
1129 ## Rooted; includes branch lengths.
```

1130 We'll pass our liolaemid tree to the `fit.bd` function, and the only additional argument to be assigned
 1131 is `rho` (for ρ), the sampling fraction, just as we did for the MCCR test in the function `mccr`. The *Reptile*
 1132 *Database* (Uetz et al. 2023) puts the total species richness of Liolaemidae at 341, so we can set `rho` to
 1133 have a value equal to the number of tips in our tree divided by this quantity.

```
liolaemid.rho <- Ntip(liolaemid.tree) / 341
liolaemid.bd <- fit.bd(liolaemid.tree, rho=liolaemid.rho)
liolaemid.bd
```

```
1134 ##
1135 ## Fitted birth-death model:
1136 ##
1137 ## ML(b/lambda) = 0.352
1138 ## ML(d/mu) = 0.1781
1139 ## log(L) = 526.451
1140 ##
1141 ## Assumed sampling fraction (rho) = 0.7537
1142 ##
1143 ## R thinks it has converged.
```

Other R packages (such as the aforementioned *diversitree*) might allow us to compare our fitted birth-death model to a range of other hypotheses about diversification, such as that the speciation and extinction rates change through time or as a function of our phenotypic traits (e.g., Maddison et al. 2007; FitzJohn 2010; Morlon et al. 2010; Revell and Harmon 2022). In *phytools* we can compare our fitted birth-death model to only one alternative model: the simpler, pure-birth model – also called a ‘Yule’ model.

```
liolaemid.yule<-fit.yule(liolaemid.tree,
  rho=liolaemid.rho)
liolaemid.yule
```

```
##
## Fitted Yule model:
##
## ML(b/lambda) = 0.2502
## log(L) = 521.1832
##
## Assumed sampling fraction (rho) = 0.7537
##
## R thinks it has converged.
```

```
anova(liolaemid.yule,liolaemid.bd)
```

```
##              log(L) d.f.      AIC      weight
## liolaemid.yule 521.1832    1 -1040.366 0.01381943
## liolaemid.bd   526.4510    2 -1048.902 0.98618057
```

This result tells us that, in the context of the two very simple models that we’ve fit to our reconstructed tree, a two-parameter birth-death (speciation and extinction) model is much better supported than our simpler Yule model!

Lastly, the *phytools* function `fit.bd` exports a likelihood function as part of the fitted model object. This, in turn, makes it very straightforward for *phytools* users to (for example) compute and graph the likelihood surface. Here, I’ll illustrate this using the base R graphics function `persp`. (But R and contributed R packages contain lots of even fancier 3D plotting methods that readers might be more interested in trying!)

```
ngrid<-40
b<-seq(0.25,0.45,length.out=ngrid)
d<-seq(0.10,0.25,length.out=ngrid)
logL<-matrix(NA,ngrid,ngrid)
for(i in 1:ngrid) for(j in 1:ngrid)
  logL[i,j]<-liolaemid.bd$lik(c(b[i],d[j]))
logL[is.nan(logL)]<-min(logL[!is.nan(logL)])
par(mar=rep(0.1,4))
persp(b,d,exp(logL),shade=0.3,phi=45,theta=20,
  xlab="speciation rate",ylab="extinction rate",
  zlab="likelihood",border=palette()[4],expand=0.3)
```

Some astute readers will notice the line `logL[is.nan(logL)] <- min(...)` (etc.) in my script of above. This is because during our grid evaluation of the likelihood function, sometimes the function was being evaluated in parameter space where the likelihood is not defined. To account for this I set all parts of the likelihood surface that could not be computed to the numerical minimum of the graph!

Figure 18 shows the very strong *ridge* in the likelihood surface (from low λ and low μ , to high λ and high μ) that almost invariably tends to characterize the likelihood surfaces of birth-death models.

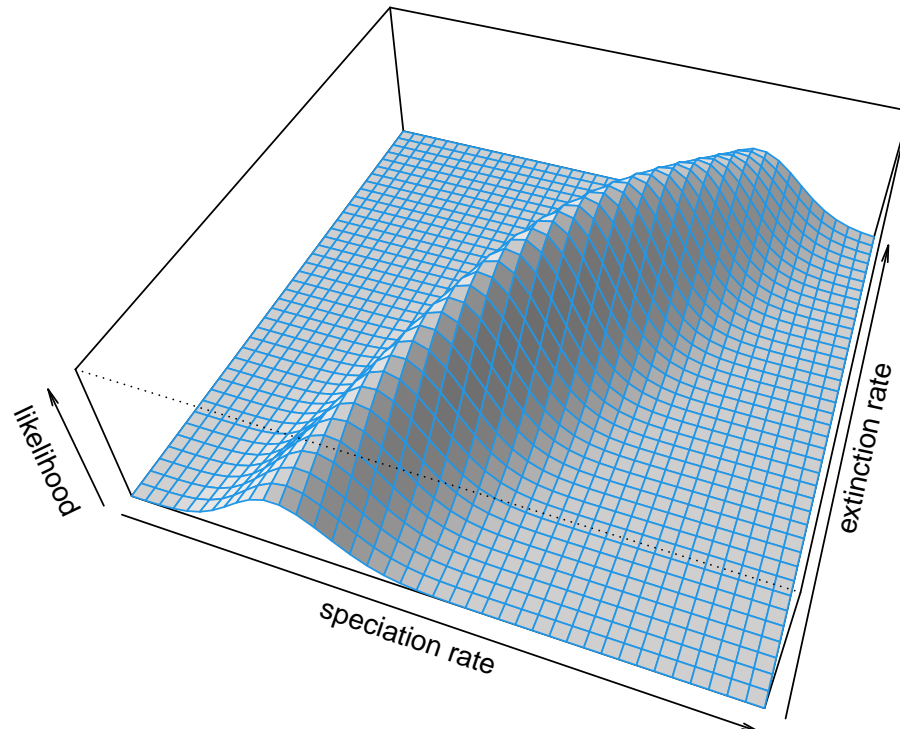


Figure 18. Visualization of the likelihood surface for speciation and extinction rates estimated for a phylogenetic tree of Liolaemidae. The ridge of values with similar likelihoods is typical of this class of model. Phylogenetic tree from Esquerré et al. (2019). See main text for more details.

7 VISUALIZATION

After phylogenetic comparative analysis, *phytools* is perhaps best known for its phylogeny visualization methods, and we’ve seen a number of these approaches already deployed throughout this article. For example, in Figures 1, 2, 3, 4, 7, and 13 I illustrated custom *phytools* plotting methods for stochastic character mapping and the analysis of stochastically mapped trees. Likewise, in Figures 5, 6, and 9 I demonstrated *phytools* plotting methods for fitted discrete character evolution models. In Figures 10, 11, 14, and 15 I showed a variety of custom methods for visualizing continuous trait evolution. Finally, in Figures 8, 16, and 17 I illustrated several different approaches for graphing diversification or the results from an analysis of diversification on the tree. This is a sparse sample of the variety of plotting methods for phylogenies, phylogenetic comparative data, and the results of phylogenetic analysis that are implemented in the *phytools* package.

In this final section, I’ll illustrate just a few more popular plotting methods of the package that we haven’t already seen in prior bits of the present article.

7.1 Co-phylogenetic plotting

Among the most popular plotting method of the *phytools* package is the function `cophylo`, which creates co-phylogenetic plots (often referred to as “tanglegrams,” Page 1993).

The purpose of tanglegrams varies widely from study to study. Classically, for instance, tanglegrams have been used to visually illustrate the topological similarity between two groups that are hypothesized to co-speciate: for instance, an animal host and its parasites, or a plant and its pollinators (e.g., Page 1993; Medina and Langmore 2016; Endara et al. 2018; Caraballo 2022).

Equally often, however, tanglegrams are put to different purposes. For instance, tanglegrams are frequently employed to show the similarity or differences between alternative phylogenetic hypotheses (e.g., Amarasinghe et al. 2021), to identify incongruence among gene trees (e.g., Stull et al. 2020), and even to compare a phylogenetic history to a non-phylogenetic cluster dendrogram based on phenotypic or ecological data (e.g., Atkinson et al. 2020; Huie et al. 2021). To illustrate the *phytools* tanglegram

1201 method, I'll use a phylogenetic tree of bat species and another of their betacoronaviruses – both based on
1202 Caraballo (2022).

```
data(bat.tree)
data(betaCoV.tree)
```

1203 Assuming that our tip labels differ between our different trees (and they do in this instance), we need
1204 more than just two phylogenies to create a tanglegram – we also need a table of associations linking the
1205 tip labels of one tree to those of the other! Again, based on Caraballo (2022), our association information
1206 for the two trees that we've loaded is contained in the *phytools* data object `bat_virus.data`. Let's
1207 load and review it.

```
data(bat_virus.data)
head(bat_virus.data)
```

```
1208 ##                Bats betaCoVs
1209 ## 1  Artibeus lituratus KT717381
1210 ## 2 Artibeus planirostris MN872692
1211 ## 3 Artibeus planirostris MN872690
1212 ## 4 Artibeus planirostris MN872691
1213 ## 5 Artibeus planirostris MN872689
1214 ## 6 Artibeus planirostris MN872688
```

1215 Inspecting just the first part of this object reveals its general structure. We can see that it consists of
1216 two columns: one for each of our two trees. The elements of the first column should match the labels of
1217 our first tree, and those of the second column the labels of our second tree. There's no problem at all if
1218 one or the other column has repeating names: a host can (of course) be associated with more than one
1219 parasite, and vice versa!

1220 Now let's run our co-phylogenetic analysis. This will create, not a plot, but a "cophylo" object in
1221 which the node rotation has been optimized to maximize the tip alignment of the two trees.

```
bat.cophylo<-cophylo(bat.tree,betaCoV.tree,
  assoc=bat_virus.data)
```

```
1222 ## Rotating nodes to optimize matching...
1223 ## Done.
```

1224 We can print this object, as follows.

```
bat.cophylo
```

```
1225 ## Object of class "cophylo" containing:
1226 ##
1227 ## (1) 2 (possibly rotated) phylogenetic trees in an object of class
1228 ##      "multiPhylo".
1229 ##
1230 ## (2) A table of associations between the tips of both trees.
```

1231 To plot it, we'll use the a generic *phytools* `plot` method for the object class. I'll go ahead and adjust
1232 a few settings of the method to make our graph look nice – and I'll use species-specific linking line colors
1233 so that we can more easily visualize all the different virus sequences that are associated with each bat
1234 host! (My color palette comes from the *RColorBrewer* function `brewer.pal`, Neuwirth 2022. I chose
1235 to use *RColorBrewer* here, rather than the *viridis* palette from earlier in the article, because it creates
1236 aesthetic *divergent* color palettes – whereas *viridis* will create a color *gradient*. *RColorBrewer* can be
1237 installed from CRAN in the typical way.)

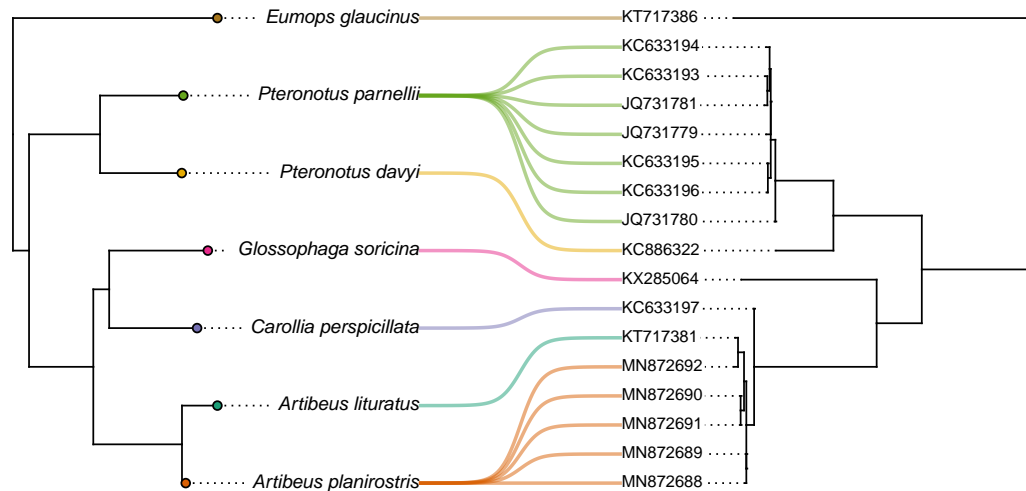


Figure 19. Co-phylogenetic plot of bat species (left) and their associated betacoronaviruses (right, labeled by GenBank accession number). Associations and GenBank accession numbers from Caraballo (2022). See main text for more details.

```
cols<-setNames(RColorBrewer::brewer.pal(n=7,
  name="Dark2"),bat.tree$tip.label)
par(lend=3)
plot(bat.cophylo,link.type="curved",fsize=c(0.7,0.6),
  link.lwd=2,link.lty="solid",pts=FALSE,
  link.col=make.transparent(cols[bat.virus.data[,1]],
    0.5),ftype=c("i","reg"))
pies<-diag(1,Ntip(bat.tree))
colnames(pies)<-rownames(pies)<-names(cols)
tiplabels.cophylo(pie=pies,
  piecol=cols[bat.cophylo$trees[[1]]$tip.label],
  which="left",cex=0.2)
```

In general, our plot reveals a surprisingly strong association between the topology of the phylogenies of the bats and their viruses – a pattern that Caraballo (2022) also reported (and that happened to contrast with what Caraballo found for alphacoronaviruses, for what it's worth).

7.2 Projecting a tree onto a geographic map

phytools can also be used to project a phylogenetic tree onto a geographic map, a visualization technique that's been used in numerous published studies since it was added to the package (e.g., Csoz and Fisher 2016; Quach et al. 2019; Hermanson et al. 2020; Huang and Morgan 2021; Osuna-Mascaró et al. 2023)

To see how this is done in R, we'll load two datasets that come with the *phytools* package. The first is a phylogenetic tree of Galapagos giant tortoises (genus *Chelonoidis*, *tortoise.tree*) based on nucleotide sequence data published Poulakakis et al. (2020). The second is a corresponding geographic dataset that I obtained from Figure 1 of the same study (Poulakakis et al. 2020).

```
data(tortoise.tree)
data(tortoise.geog)
```

Our geographic data (*tortoise.geog*), which contain latitude and longitude measures in two columns, can be a data frame or matrix. In the event that any of the operational taxa of our tree are represented more than once in our geographic data, then our coordinate data *must* take the form of a matrix. This is important to note because our plotting function requires that our taxon labels be supplied as row names. The most common ways to read data into R (for instance, using *read.table* or *read.csv*)

1254 create data frames, rather than a matrices – and R data frames don’t permit repeating row names! In the
1255 case of our tortoise data, the labels of our data and tree match without duplication, so our input data can
1256 be provided in either acceptable format.

1257 Let’s review our locality data frame, `tortoise.geog`, to understand precisely how it’s been
1258 structured.

```
tortoise.geog
```

```
1259 ##               lat      long
1260 ## C._duncanensis_1 -0.611014 -90.66008
1261 ## C._abingdonii    0.583058 -90.75376
1262 ## C._niger         -1.291984 -90.42749
1263 ## C._vicina_1      -0.915375 -91.38897
1264 ## C._chathamensis -0.818184 -89.41856
1265 ## C._becki         0.031506 -91.39121
1266 ## C._darwini       -0.268896 -90.70471
1267 ## C._donfaustoi    -0.642738 -90.20561
1268 ## C._hoodensis     -1.378876 -89.67889
1269 ## C._duncanensis_2 -0.611014 -90.66008
1270 ## C._porteri       -0.697202 -90.48687
1271 ## C._vicina_2      -0.915375 -91.38897
1272 ## C._guntheri      -0.800044 -91.03839
1273 ## C._vanderburghi -0.447016 -91.10362
1274 ## C._microphyes    -0.250360 -91.32202
```

1275 We should see that it consists of species names as row names, as promised, and geographic locality
1276 points in the form of decimal latitude (in the first column) and longitude (in the second) coordinates.

1277 Our next step will be to build the map projection that we intend to plot. This is done using the
1278 *phytools* function `phylo.to.map`. In addition to combining our phylogenetic tree and map data,
1279 `phylo.to.map`, much like the `cophylo` method of the previous section, performs a series of node
1280 rotations designed to optimize the alignment of our phylogeny with the geographic coordinates of our tip
1281 data. As node rotation is arbitrary anyway, this can be helpful to facilitate a more convenient visualization.

1282 Before running this code section, we’ll load the R package *mapdata* (Becker et al. 2022b, which
1283 can be installed from CRAN in the usual way). This will allow us to access a higher resolution base
1284 map of the geographic region we intend to plot. We should also specify `direction="rightwards"`.
1285 This indicates that we intend to graph our phylogeny to the *left* of our plotted map facing *right*, and thus
1286 permits `phylo.to.map` to optimize its node rotations of the tree accordingly.

```
library(mapdata)
tortoise.phymap<-phylo.to.map(tortoise.tree,
  tortoise.geog,plot=FALSE,direction="rightwards",
  database="worldHires",regions="Ecuador")
```

```
1287 ## objective: 64
```

```
1288 ## objective: 52
```

```
1289 ## objective: 52
```

```
1290 ## objective: 52
```

```
1291 ## objective: 52
```

```
1292 ## objective: 52
```

```
1293 ## objective: 52
```

```
1294 ## objective: 52
```

```
1295 ## objective: 52
```

```
1296 ## objective: 46
```

```
1297 ## objective: 46
```

```
1298 ## objective: 46
```

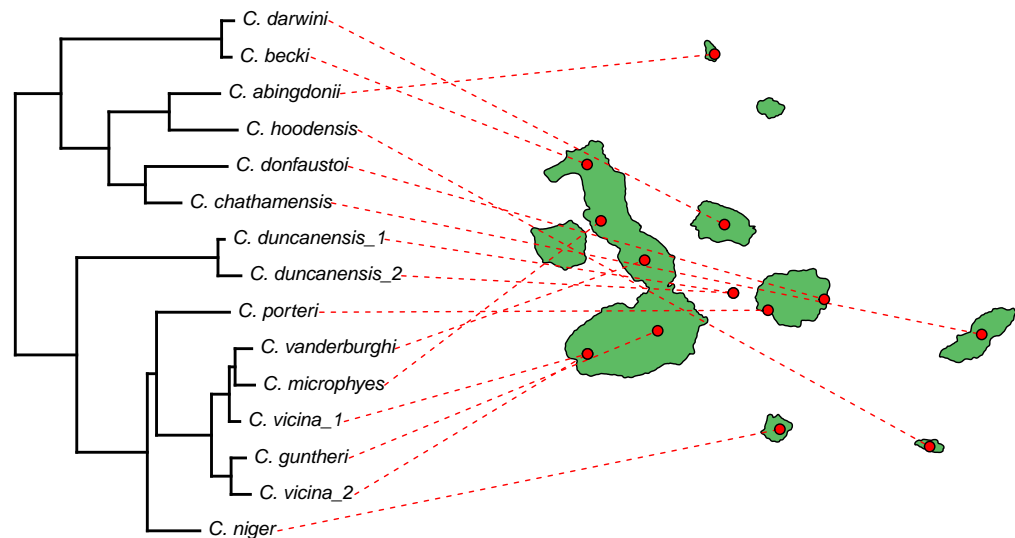


Figure 20. A phylogenetic tree of Galapagos tortoises projected onto a geographic map. Phylogenetic data and geographic locality information are based on Poulakakis et al. (2020). See main text for more details.

```
1299 ## objective: 44
1300 ## objective: 44
```

1301 The object we've created is of class "phylo.to.map" and contains both our optimized tree, the
1302 geographic coordinates of our observations, and our underlying base map for plotting.

```
tortoise.phymap
```

```
1303 ## Object of class "phylo.to.map" containing:
1304 ##
1305 ## (1) A phylogenetic tree with 15 tips and 14 internal nodes.
1306 ##
1307 ## (2) A geographic map with range:
1308 ##     -5.01N, 1.44N
1309 ##     -91.67W, -75.22W.
1310 ##
1311 ## (3) A table containing 15 geographic coordinates (may include
1312 ##     more than one set per species).
1313 ##
1314 ## If optimized, tree nodes have been rotated to maximize alignment
1315 ## with the map when the tree is plotted in a rightwards direction.
```

1316 Finally, we're ready to plot our tree. Here, we must remember to specify the *x* and *y* axis limits (via
1317 the arguments *xlim* and *ylim*, respectively) based on the geographic coordinates of our geolocality
1318 data.

```
plot(tortoise.phymap, direction="rightwards", pts=FALSE,
     xlim=c(-92.25, -89.25), ylim=c(-1.8, 0.75), ftype="i",
     fsize=0.8, lty="dashed", map.bg="#5dbb63")
```

1319 Although the base map from *mapdata* is sufficiently high resolution for our purposes here, higher
1320 resolution maps are available for some regions, and it's even possible to import and use a custom map –
1321 should we be so inclined (e.g., Quach et al. 2019).

7.3 Projecting trees into phenotypic space

Along with projecting a phylogenetic tree onto a geographic map (as we just saw), and projecting traits onto the edges and nodes of a plotted tree, the *phytools* package also contains multiple methods to project a tree into a space defined by our traits. Undoubtedly, the most popular of these are *phylomorphospace*, which projects a tree into a bivariate quantitative trait space (Sidlauskas 2008; e.g., Friedman et al. 2016; Martins et al. 2021), and *phenogram*, which projects a tree into a space defined by time since the root on the horizontal and phenotype on the vertical (typically called a “traitgram,” see Evans et al. 2009; e.g., Martinez et al. 2020; Chazot et al. 2021). We saw how *phenogram* works in Figure 14b of any earlier section of this article. Here, I’ll focus on the *phytools* method *phylomorphospace*.

For this example I’ll be using a time-calibrated phylogeny of 11 vertebrate species from the *TimeTree* website (Hedges et al. 2006), and a phenotypic trait dataset of body mass (in kg) and mean litter size. (The latter dataset was generated from *Wikipedia* and other sources: i.e., “Googling it.”)

```
data(vertebrate.tree)
data(vertebrate.data)
head(vertebrate.data)
```

```
##           Mass Length Litter_size
## Carcharodon_carcharias 2268.00   6.100      10.0
## Carassius_auratus      0.91   0.380     200.0
## Latimeria_chalumnae    80.00   2.000      15.0
## Iguana_iguana          8.00   2.000      50.5
## Turdus_migratorius      0.28   0.094       4.0
## Homo_sapiens           80.00   1.700       1.1
```

We should see that our data frame actually has three columns – but henceforward I’ll just use the first and the third of these.

Normally, we could pass our data frame or matrix and phylogeny directly to the *phylomorphospace* function and obtain a plot. *phylomorphospace* would then undertake to project the tree, using Maximum Likelihood reconstructed ancestral values for both traits as the positions for internal nodes. In this case, however, I’d prefer to first reconstruct ancestral states on a log scale, back-transform my estimated values to the original space, and then use these back-transformed reconstruction as my node positions. Fortunately, *phylomorphospace* allows that! (In addition to the reasoning I provided in an earlier section, the logic of reconstructing ancestral states on a log scale is because quantitative traits in general, and morphometric data in particular, often satisfy the Brownian motion assumption better on a logarithmic than linear scale. The reasoning of back-transforming before plotting or reporting our results is simply because most human brains, mine included, are more adept at interpreting values on an additive rather than multiplicative scale!)

For the first step, I’ll use the *phytools* ancestral state estimation function *fastAnc*. *fastAnc* computes Maximum Likelihood ancestral states for one input character vector at a time, so we just need to iterate across the two columns (of interest) in our data frame using an *apply* call as follows.

```
vertebrate.ace<-exp(apply(log(vertebrate.data[,c(1,3)]),
  2,fastAnc,tree=vertebrate.tree))
vertebrate.ace
```

```
##           Mass Litter_size
## 12  25.571594  15.552422
## 13  17.834793  16.114126
## 14  16.827622  14.481309
## 15   8.801275   8.791375
## 16  20.362215   1.653955
## 17  17.335294   1.442396
## 18  24.604666   1.610416
## 19 152.078728   1.737334
## 20 301.219076   1.582780
## 21   6.329908   9.613237
```

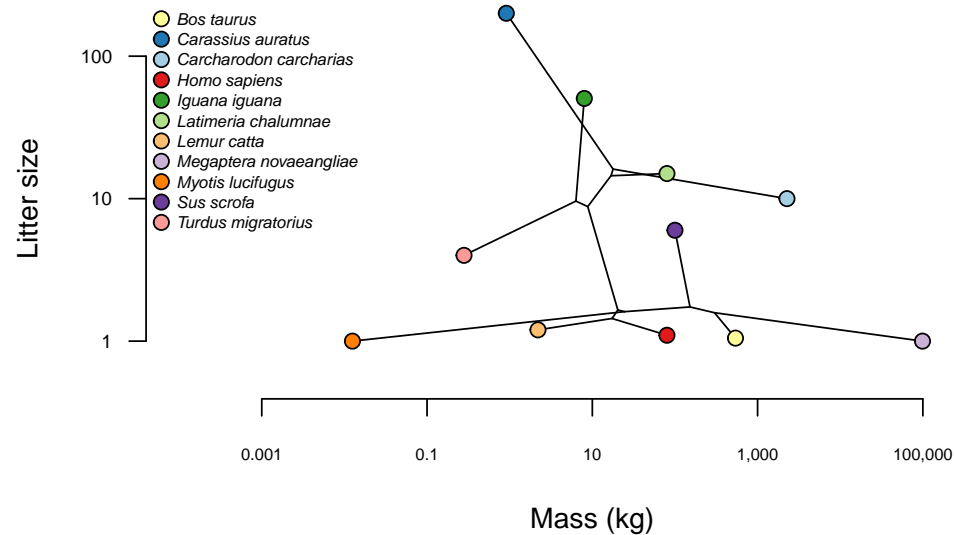


Figure 21. Phylomorphospace of body mass and litter size for a selection of vertebrate species. The underlying phylogenetic tree was obtained from Hedges et al. (2006). See main text for additional details.

1368 This gives us a set of reconstructed values on our original (linear) scale, but in which the reconstruction
1369 was performed on a *log* scale, and then back-transformed. Finally, let's create our phylomorphospace plot.

```
par(mar=c(5.1, 4.1, 0.6, 2.1))
phylomorphospace(vertebrate.tree,
  vertebrate.data[,c(1,3)], A=vertebrate.ace, log="xy",
  xlim=c(1e-4, 1e6), ylim=c(0.5, 200), bty="n", label="off",
  axes=FALSE, xlab="Mass (kg)", ylab="Litter size",
  node.size=c(0,0))
axis(1, at=10^seq(-3, 5, by=2),
  labels=prettyNum(10^seq(-3, 5, by=2), big.mark=","),
  las=1, cex.axis=0.6)
axis(2, at=10^seq(0, 2, by=1),
  labels=prettyNum(10^seq(0, 2, by=1), big.mark=","),
  las=1, cex.axis=0.7)
cols<-setNames(RColorBrewer::brewer.pal(
  nrow(vertebrate.data), "Paired"),
  rownames(vertebrate.data))
points(vertebrate.data[,c(1,3)], pch=21, bg=cols, cex=1.2)
ind<-order(rownames(vertebrate.data))
legend("topleft", gsub("-", " ",
  rownames(vertebrate.data))[ind], pch=21, pt.cex=1.2,
  pt.bg=cols[ind], cex=0.6, bty="n", text.font=3)
```

1370 Here, I chose to graph the projection without taxon labels, then add different colored points and a
1371 legend to put the label information back on the plot (sorting my labels alphabetically as I did this). As
1372 readers can probably imagine, taxon labels on a phylomorphospace plot can easily become very messy –
1373 particularly for larger trees!

1374 7.4 Plotting phenotypic data at the tips of the tree

1375 In addition to projecting phylogenies into trait spaces, and plotting observed or reconstructed trait values
1376 on the tree, *phytools* possesses a number of different plotting methods that can also help us undertake the
1377 (at least, conceptually) simple task of visualizing comparative trait data for species at the tips of the tree.

This might be done in various ways. For instance, we could graph the values of a quantitative trait adjacent to the tip labels using a bar or box, or we might plot the presence or absence of different lineages from a habitat type next to the tips of the tree (Revell 2014b). Numerous such approaches have been developed and implemented in the *phytools* package, and many of these are shown in my recent book (Revell and Harmon 2022).

Here, I'll illustrate just one such method in which a color gradient is used to visualize trait values for a set of quantitative characters at the tips of the tree (Revell 2014b). The *phytools* implementation of this plotting method is called `phylo.heatmap`, and it's been used in numerous published articles (e.g., Goelen et al. 2020; Hultgren et al. 2021; Molina-Mora et al. 2021; Huang et al. 2022; Morales-Poole et al. 2022). For this example, we'll use a phylogenetic tree and log-transformed morphological trait dataset for *Anolis* lizards from (Mahler et al. 2010). To load these data, readers should run the following.

```
data(anoletree)
data(anole.data)
head(anole.data)
```

```
##              SVL      HL      HLL      FLL      LAM      TL
## ahli          4.03913 2.88266 3.96202 3.34498 2.86620 4.50400
## allogus       4.04014 2.86103 3.94018 3.33829 2.80827 4.52189
## rubribarbus   4.07847 2.89425 3.96135 3.35641 2.86751 4.56108
## imias         4.09969 2.85293 3.98565 3.41402 2.94375 4.65242
## sagrei        4.06716 2.83515 3.85786 3.24267 2.91872 4.77603
## bremeri       4.11337 2.86044 3.90039 3.30585 2.97009 4.72996
```

Our trait data object, `anole.data`, is a data frame with six trait columns for various phylogenetic traits.

We could visualize our data directly; however, the effect of overall size (data column "SVL") would tend to obscure any interesting patterns of residual variation and covariation in body shape among the species in our tree. As such, primarily in an effort to control for overall size, I'll first run a phylogenetic principal components analysis (Revell 2009) using the *phytools* function `phyl.pca`. A phylogenetic principal components analysis (mentioned earlier with respect to the Broeckhoven et al. 2016 dataset) is similar to a regular PCA except that we account for non-independence of the information for different species in our data rotation (Revell 2009).

```
anole.pcca <- phyl.pca(anoletree, anole.data, mode="corr")
anole.pcca
```

```
## Phylogenetic pca
## Standard deviations:
##      PC1      PC2      PC3      PC4      PC5      PC6
## 2.2896942 0.6674345 0.4381067 0.2997973 0.1395612 0.1026573
## Loads:
##      PC1      PC2      PC3      PC4      PC5
## SVL -0.9782776 -0.01988115 0.14487425 -0.11332244 0.0781070110
## HL  -0.9736568 -0.03879982 0.13442473 -0.15596460 -0.0852979941
## HLL -0.9711545 0.14491400 0.02151524 0.17058611 -0.0588208480
## FLL -0.9759133 -0.02087140 0.14486273 0.14149988 0.0475205990
## LAM -0.8299594 -0.50437051 -0.23796010 0.01194704 0.0004983465
## TL  -0.8679195 0.40956428 -0.27350654 -0.05871034 0.0195584629
##      PC6
## SVL -0.051442939
## HL  0.028570939
## HLL -0.053257988
## FLL 0.062386141
## LAM -0.003133966
## TL  0.018373275
```


Our PC loadings show us the the first principal component dimension is strongly negatively correlated with all of the traits in our analysis. We could consider this the “size” axis. Principal component 2 is most strongly (negatively) correlated with the character “LAM”, number of adhesive toepad scales called lamellae; and most positively correlated with “TL”, tail length.

Let’s compute the principal component scores for all of our species.

```
anole.pc.scores<-scores(anole.pPCA)
head(anole.pc.scores)
```

```
##          PC1          PC2          PC3          PC4          PC5
## ahli      -0.1747576  0.8697064  1.52379491  1.6029659 -0.23955421
## allogus    0.1646585  1.4017806  1.74506491  1.5358005 -0.08089546
## rubribarbus -0.4925001  1.0413268  1.45866163  1.4180850 -0.05716104
## imias     -1.1608049  0.7514380  0.75822327  1.7127381  0.35013533
## sagrei     -0.3486332  1.2632997 -0.05102313  0.7317455  0.37217463
## bremeri    -0.9714818  0.6943196  0.11689334  0.9290039  0.43486041
##
##          PC6
## ahli      -0.1626049
## allogus    -0.1245855
## rubribarbus -0.1797060
## imias     -0.1340347
## sagrei     -0.1484157
## bremeri    -0.2304513
```

Since the sign of each principal component is arbitrary (principal components are vectors), we’ll now “flip” the sign of PC 1 – so that it switches from negative size to simply “size.”

```
anole.pc.scores[,1]<- -anole.pc.scores[,1]
head(anole.pc.scores)
```

```
##          PC1          PC2          PC3          PC4          PC5
## ahli      0.1747576  0.8697064  1.52379491  1.6029659 -0.23955421
## allogus   -0.1646585  1.4017806  1.74506491  1.5358005 -0.08089546
## rubribarbus 0.4925001  1.0413268  1.45866163  1.4180850 -0.05716104
## imias      1.1608049  0.7514380  0.75822327  1.7127381  0.35013533
## sagrei      0.3486332  1.2632997 -0.05102313  0.7317455  0.37217463
## bremeri      0.9714818  0.6943196  0.11689334  0.9290039  0.43486041
##
##          PC6
## ahli      -0.1626049
## allogus    -0.1245855
## rubribarbus -0.1797060
## imias     -0.1340347
## sagrei     -0.1484157
## bremeri    -0.2304513
```

Finally, let’s graph our results using the `phylo.heatmap` function. Seeing as the variance in our different principal component dimensions are quite different from PC to PC, we’ll standardize them to have a constant variance using `standardize=TRUE`. As we’ve done in other exercises of this article, we can update the default color palette of the plot using the argument `colors`. Here, I’ll use the colorblind-friendly viridis color palette from the *viridisLite* package (Garnier et al. 2022) that we learned about earlier.

```
phylo.heatmap(anoletree, anole.pc.scores,
  standardize=TRUE, fsize=c(0.4, 0.7, 0.7), pts=FALSE,
  split=c(0.6, 0.4), colors=viridisLite::viridis(n=40,
  direction=-1), mar=rep(0.1, 4))
```

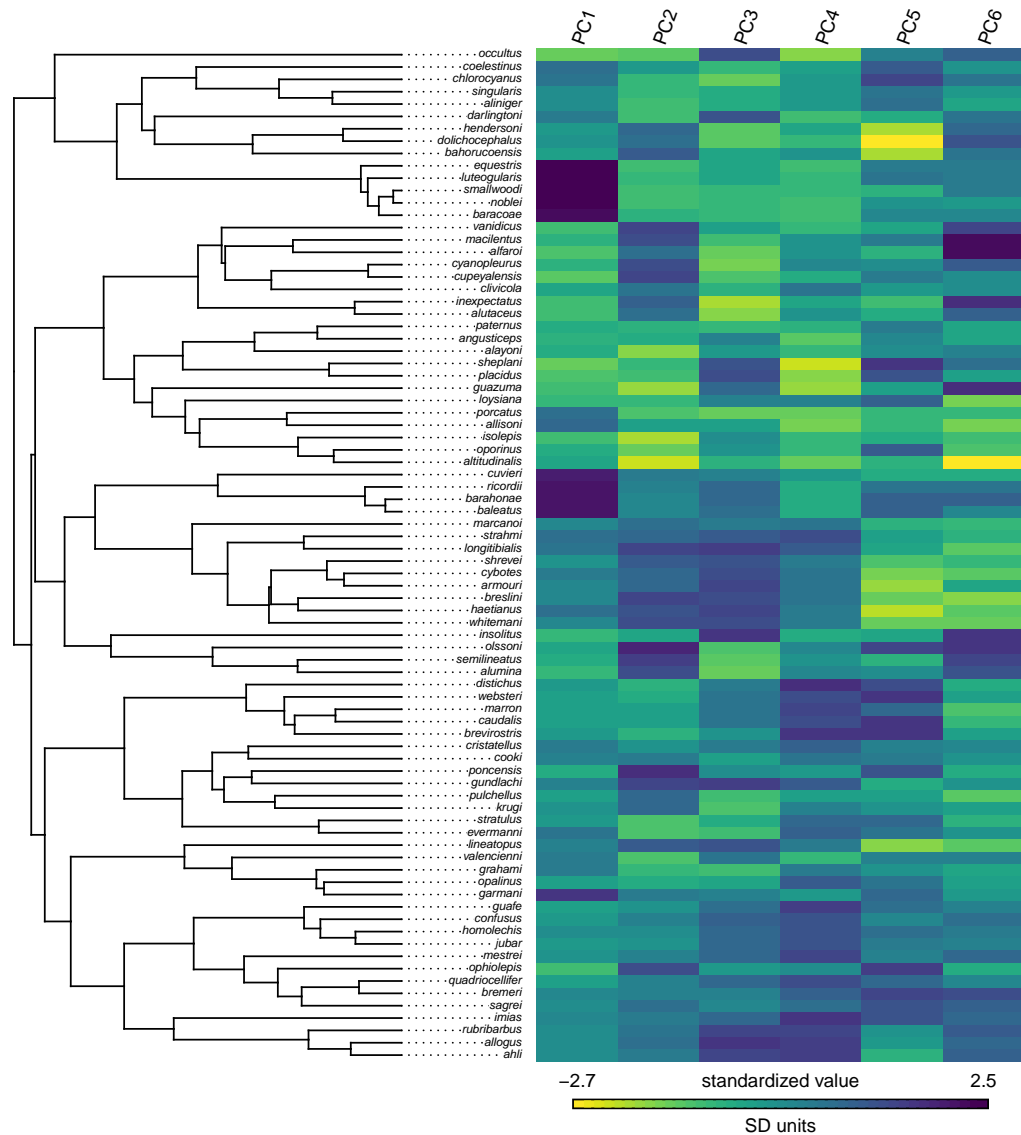


Figure 22. Phylogenetic heatmap showing principal components from a phylogenetic PCA of six morphological traits of *Anolis* lizards. Tree and data are from Mahler et al. (2010). See main text for additional details.

In Figure 22 we can already begin to discern some of the interesting ecomorphological phenotypic patterns of *Anolis* lizards (Losos 2009). For instance, the largest species (known as “crown-giants,” Losos 2009), that is, those species with the highest values of PC 1, tend to have moderate or low values for PC 2: meaning they have larger lamellae and shorter tails, controlling for their body size. By contrast some of the smallest species (on PC 1) have among the highest values for PC 2 (tail length). These are the “grass-bush” anoles that perch on grass and bushes near the grown, and use their long tails to control body pitch while jumping. We can likewise see that this combination of phenotypic traits (large body size and large lamellae; small body size and long tail) has evolved *independently* in different parts of the phylogenetic tree. Just by visualizing our data and learning this, we’re already doing phylogenetic comparative methods. Neat!

8 RELATIONSHIP OF *PHYTOOLS* TO OTHER PACKAGES

The *phytools* package has grown to become (along with *ape*, *phangorn*, and *geiger*) among the most important core packages for phylogenetic analysis in the R environment. As of the time of writing, the original publication describing *phytools* (Revell, 2012) had been cited more than 7,300 times on *Google Scholar* and continues to be cited over 1,000 times per year.

In many respect, however, *phytools* owes its existence to a number of other packages making up the R phylogenetics ecosystem and from which it imports critical functionality. In particular, *phytools* depends on the object classes and methods of the core R phylogenetics package, *ape* (Paradis et al. 2004; Popescu et al. 2012; Paradis and Schliep 2019). In addition, *phytools* relies on a number of different methods from the multifunctional phylogenetic inference package, *phangorn* (Schliep 2011). Finally, *phytools* is designed to interact with a variety of other function R phylogenetics libraries, especially the *geiger* package (Harmon et al. 2008; Pennell et al. 2014), which *phytools* “suggests” but does not import.

Outside phylogenetics as such, *phytools* also presently depends on or imports from a number of other R packages including *clusterGeneration* (Qiu and Joe. 2020), *coda* (Plummer et al. 2006), *combinat* (Chasalow 2012), *doParallel* (Corporation and Weston 2022), *expm* (Maechler et al. 2023), *foreach* (Microsoft and Weston 2022), *maps* (Becker et al. 2022a), *MASS* (Venables and Ripley 2002), *mnormt* (Azzalini and Genz 2022), *nlme* (Pinheiro and Bates 2000; Pinheiro et al. 2022), *numDeriv* (Gilbert and Varadhan 2019), *optimParallel* (Gerber and Furrer 2019), *plotrix* (J 2006), and *scatterplot3d* (Ligges and Mächler 2003), although dependency relationships are dynamic as packages evolve and may change.

9 CONCLUSIONS

More than a decade has passed since the original and only article describing *phytools* was published (Revell 2012). Since that time, the *phytools* package has both evolved into one of the core function libraries of the R phylogenetics ecosystem, and expanded manyfold in size and scope. As such, I decided the literature reference for *phytools* was sorely in need of updating. In creating one, however, I was determined to make something that could serve as more than a placeholder to capture citations of the *phytools* package. I hope that what I’ve provided here will help guide some new *phytools* users towards interesting analytical tools, as well as perhaps inspire experienced *phytools* and R phylogenetics researchers to generate new types of questions and data that will in turn help motivate continued development of the *phytools* package into the future.

10 SOFTWARE AND DATA AVAILABILITY

The *phytools* R package is free and open source, and can be downloaded from its CRAN (<https://CRAN.R-project.org/package=phytools>) or GitHub (<https://github.com/liamrevell/phytools>) pages. More information about the *phytools* package can be obtained from the software documentation pages, my *phytools* blog (<http://blog.phytools.org>), or via my recent book with Luke Harmon (Revell and Harmon 2022).

This article was written in Rmarkdown (Xie et al. 2018, 2020; Allaire et al. 2023), and developed with the help of both *bookdown* (Xie 2016, 2023) and the posit Rstudio IDE (RStudio Team 2020). Markdown code and data files necessary to exactly reproduce the analyses of this article are available at <https://github.com/liamrevell/Revell.phytools-v2/> (and folders therein).

REFERENCES

- 1514
- 1515 Allaire, J., Y. Xie, J. McPherson, J. Luraschi, K. Ushey, A. Atkins, H. Wickham, J. Cheng, W. Chang, and
- 1516 R. Iannone. 2023. Rmarkdown: Dynamic documents for R.
- 1517 Amarasinghe, P., S. Joshi, N. Page, L. S. Wijedasa, M. Merello, H. Kathriarachchi, R. D. Stone, W. Judd,
- 1518 U. Kodandaramaiah, and N. Cellinese. 2021. Evolution and biogeography of memecylon. *Am. J. Bot.*
- 1519 108:628–646. Wiley.
- 1520 Atkinson, C. L., B. C. Ee, and J. M. Pfeiffer. 2020. Evolutionary history drives aspects of stoichiometric
- 1521 niche variation and functional effects within a guild. *Ecology* 101:e03100. Wiley.
- 1522 Azzalini, A., and A. Genz. 2022. The R package *mnormt*: The multivariate normal and *t* distributions
- 1523 (version 2.1.1).
- 1524 Baele, G., S. Dellicour, M. A. Suchard, P. Lemey, and B. Vrancken. 2018. Recent advances in computa-
- 1525 tional phylodynamics. *Curr. Opin. Virol.* 31:24–32. Elsevier BV.
- 1526 Bartoszek, K., J. Pienaar, P. Mostad, S. Andersson, and T. F. Hansen. 2012. A phylogenetic comparative
- 1527 method for studying multivariate adaptation. *Journal of Theoretical Biology* 314:204–215.
- 1528 Bastide, P., C. Ané, S. Robin, and M. Mariadassou. 2018. Inference of adaptive shifts for multivariate
- 1529 correlated traits. *Systematic Biology* 67:662–680. Oxford University Press (OUP).
- 1530 Beale, M. A., M. Marks, S. K. Sahi, L. C. Tantalo, A. V. Nori, P. French, S. A. Lukehart, C. M. Marra,
- 1531 and N. R. Thomson. 2019. Genomic epidemiology of syphilis reveals independent emergence of
- 1532 macrolide resistance across multiple circulating lineages. *Nat. Commun.* 10:3255. Springer Science;
- 1533 Business Media LLC.
- 1534 Beaulieu, J. M., and B. C. O’Meara. 2016. Detecting hidden diversification shifts in models of trait-
- 1535 dependent speciation and extinction. *Systematic Biology* 65:583–601.
- 1536 Beaulieu, J. M., B. C. O’Meara, and M. J. Donoghue. 2013. Identifying hidden rate changes in the
- 1537 evolution of a binary morphological character: The evolution of plant habit in campanulid angiosperms.
- 1538 *Syst. Biol.* 62:725–737.
- 1539 Beaulieu, J., B. O’Meara, J. Oliver, and J. Boyko. 2022. *corHMM*: Hidden Markov models of character
- 1540 evolution.
- 1541 Becker, R. A., A. R. Wilks, R. Brownrigg, T. P. Minka, and A. Deckmyn. 2022a. *Maps*: Draw geographical
- 1542 maps.
- 1543 Becker, R. A., A. R. Wilks, and R. Brownrigg. 2022b. *Mapdata*: Extra map databases.
- 1544 Bentz, C., D. Dediu, A. Verkerk, and G. Jäger. 2018. The evolution of language families is shaped by the
- 1545 environment beyond neutral drift. *Nat. Hum. Behav.* 2:816–821. Springer Science; Business Media
- 1546 LLC.
- 1547 Blinkhorn, J., and M. Grove. 2021. Explanations of variability in Middle Stone Age stone tool assemblage
- 1548 composition and raw material use in Eastern Africa. *Archaeol. Anthropol. Sci.* 13:14. Springer
- 1549 Science; Business Media LLC.
- 1550 Blomberg, S. P., T. Garland Jr, and A. R. Ives. 2003. Testing for phylogenetic signal in comparative data:
- 1551 Behavioral traits are more labile. *Evolution* 57:717–745.
- 1552 Bollback, J. P. 2006. SIMMAP: Stochastic character mapping of discrete traits on phylogenies. *BMC*
- 1553 *Bioinformatics* 7:88. Springer Science; Business Media LLC.
- 1554 Broeckhoven, C., G. Diedericks, C. Hui, B. G. Makhubo, and P. le Fras N. Mouton. 2016. Enemy at the
- 1555 gates: Rapid defensive trait diversification in an adaptive radiation of lizards. *Evolution* 70:2647–2656.
- 1556 Wiley.
- 1557 Burnham, K. P., and D. R. Anderson. 2003. Model selection and multimodel inference: A practical
- 1558 information theoretic approach. Springer Science & Business Media.
- 1559 Bushman, F. D., K. McCormick, and S. Sherrill-Mix. 2019. Virus structures constrain transmission
- 1560 modes. *Nat. Microbiol.* 4:1778–1780. Springer Science; Business Media LLC.
- 1561 Butler, M. A., and A. A. King. 2004. Phylogenetic comparative analysis: A modeling approach for
- 1562 adaptive evolution. *Am. Nat.* 164:683–695.
- 1563 Caetano, D. S., and L. J. Harmon. 2017. Ratematrix: An R package for studying evolutionary integration
- 1564 among several traits on phylogenetic trees. *Methods in Ecology and Evolution* 8:1920–1927. Wiley.
- 1565 Caraballo, D. A. 2022. Cross-species transmission of bat coronaviruses in the americas: Contrasting
- 1566 patterns between alphacoronavirus and betacoronavirus. *Microbiol. Spectr.* 10:e0141122. American
- 1567 Society for Microbiology.
- 1568 Chasalow, S. 2012. *Combinat*: Combinatorics utilities.

- 1569 Chazot, N., P. Blandin, V. Debat, M. Elias, and F. L. Condamine. 2021. Punctuational ecological changes
1570 rather than global factors drive species diversification and the evolution of wing phenotypes in morpho
1571 butterflies. *J. Evol. Biol.* 34:1592–1607. Wiley.
- 1572 Clavel, J., G. Escarguel, and G. Merceron. 2015. MvMORPH: An R package for fitting multivariate
1573 evolutionary models to morphometric data. *Methods in Ecology and Evolution* 6:1311–1319.
- 1574 Collar, D. C., P. C. Wainwright, M. E. Alfaro, L. J. Revell, and R. S. Mehta. 2014. Biting disrupts
1575 integration to spur skull evolution in eels. *Nature* 5:5505.
- 1576 Compton, Z., V. Harris, W. Mellon, S. Rupp, D. Mallo, S. E. Kapsetaki, M. Wilmot, R. Kennington, K.
1577 Noble, C. Baci, L. Ramirez, A. Peraza, B. Martins, S. Sudhakar, S. Aksoy, G. Furukawa, O. Vincze,
1578 M. Giraudeau, E. G. Duke, S. Spiro, E. Flach, H. Davidson, A. Zehnder, T. A. Graham, B. Troan, T.
1579 M. Harrison, M. Tollis, J. D. Schiffman, A. Aktipis, L. M. Abegglen, C. C. Maley, and A. M. Boddy.
1580 2023. Cancer prevalence across vertebrates. *bioRxiv*org.
- 1581 Corporation, M., and S. Weston. 2022. doParallel: Foreach parallel adaptor for the 'parallel' package.
- 1582 Csomos, S., and B. Fisher. 2016. Taxonomic revision of the malagasy nesomyrmex madeassus species-
1583 group using a quantitative morphometric approach. *ZooKeys* 603:105–130. Pensoft Publishers.
- 1584 Damian-Serrano, A., S. H. D. Haddock, and C. W. Dunn. 2021. The evolution of siphonophore tentilla
1585 for specialized prey capture in the open ocean. *Proceedings of the National Academy of Sciences* 118.
1586 *Proceedings of the National Academy of Sciences*.
- 1587 Efron, B., and G. Gong. 1983. A leisurely look at the bootstrap, the jackknife, and cross-validation. *Am.*
1588 *Stat.* 37:36–48. Informa UK Limited.
- 1589 Endara, M.-J., J. A. Nicholls, P. D. Coley, D. L. Forrister, G. C. Younkin, K. G. Dexter, C. A. Kidner, R. T.
1590 Pennington, G. N. Stone, and T. A. Kursar. 2018. Tracking of host defenses and phylogeny during
1591 the radiation of neotropical inga-feeding sawflies (hymenoptera; argidae). *Front. Plant Sci.* 9:1237.
1592 Frontiers Media SA.
- 1593 Esquerré, D., I. G. Brennan, R. A. Catullo, F. Torres-Pérez, and J. S. Keogh. 2019. How mountains shape
1594 biodiversity: The role of the Andes in biogeography, diversification, and reproductive biology in south
1595 america's most species-rich lizard radiation (Squamata: Liolaemidae). *Evolution* 73:214–230. Wiley.
- 1596 Etienne, R. S., and B. Haegeman. 2012. A conceptual and statistical framework for adaptive radiations
1597 with a key role for diversity dependence. *Am. Nat.* 180:E75–89.
- 1598 Etienne, R. S., and B. Haegeman. 2023. DDD: Diversity-dependent diversification.
- 1599 Evans, M. E. K., S. A. Smith, R. S. Flynn, and M. J. Donoghue. 2009. Climate, niche evolution, and
1600 diversification of the “Bird-Cage” evening primroses (Oenothera, sections Anogra and Kleinia). *Am.*
1601 *Nat.* 173:225–240. The University of Chicago Press.
- 1602 Felsenstein, J. 2012. A comparative method for both discrete and continuous characters using the threshold
1603 model. *Am. Nat.* 179:145–156.
- 1604 Felsenstein, J. 2002. Graphical methods for visualizing comparative data on phylogenies. Pp. 27–44 in N.
1605 MacLeod and P. Forey, eds. *Morphology, shape and phylogeny*. Taylor; Francis, London, UK.
- 1606 Felsenstein, J. 2004. *Inferring phylogenies*. Sinauer associates, Sunderland, MA.
- 1607 Felsenstein, J. 1985. Phylogenies and the comparative method. *Am. Nat.* 125:1–15.
- 1608 Felsenstein, J. 2005. Using the quantitative genetic threshold model for inferences between and within
1609 species. *Philos. Trans. R. Soc. Lond. B Biol. Sci.* 360:1427–1434.
- 1610 FitzJohn, R. G. 2012. Diversitree : Comparative phylogenetic analyses of diversification in R. *Methods*
1611 *Ecol. Evol.* 3:1084–1092. Wiley.
- 1612 FitzJohn, R. G. 2010. Quantitative traits and diversification. *Syst. Biol.* 59:619–633. Oxford University
1613 Press (OUP).
- 1614 Freitas, A. R., A. P. Tedim, C. Novais, V. F. Lanza, and L. Peixe. 2020. Comparative genomics of global
1615 optrA-carrying Enterococcus faecalis uncovers a common chromosomal hotspot for optrA acquisition
1616 within a diversity of core and accessory genomes. *Microb. Genom.* 6:e000350. Microbiology Society.
- 1617 Friedman, S. T., S. A. Price, A. S. Hoey, and P. C. Wainwright. 2016. Ecomorphological convergence in
1618 planktivorous surgeonfishes. *J. Evol. Biol.* 29:965–978.
- 1619 Galtier, N. 2001. Maximum-likelihood phylogenetic analysis under a covarion-like model. *Molecular*
1620 *Biology and Evolution* 18:866–873.
- 1621 Garamszegi, L. Z. 2014. *Modern phylogenetic comparative methods and their application in evolutionary*
1622 *biology: Concepts and practice*. Springer.
- 1623 Garnier, Simon, Ross, Noam, Rudis, Robert, Camargo, A. Pedro, Sciaini, Marco, Scherer, and Cédric.

2022. *viridis* - Colorblind-friendly color maps for R.
- Gerber, F., and R. Furrer. 2019. OptimParallel: An R package providing a parallel version of the L-BFGS-B optimization method. *The R Journal* 11:352–358.
- Gilbert, P., and R. Varadhan. 2019. numDeriv: Accurate numerical derivatives.
- Goelen, T., I. S. Sobhy, C. Vanderaa, F. Wäckers, H. Rediers, T. Wenseleers, H. Jacquemyn, and B. Lievens. 2020. Bacterial phylogeny predicts volatile organic compound composition and olfactory response of an aphid parasitoid. *Oikos* 129:1415–1428. Wiley.
- Goldberg, E. E., and B. Igić. 2012. Tempo and mode in plant breeding system evolution. *Evolution* 66:3701–3709. Wiley Online Library.
- Halali, S., E. Bergen, C. J. Breuker, P. M. Brakefield, and O. Brattström. 2020. Seasonal environments drive convergent evolution of a faster pace-of-life in tropical butterflies. *Ecology Letters* 24:102–112. Wiley.
- Harmon, L. J. 2019. Phylogenetic comparative methods: Learning from trees. *Ecoevorxiv*.
- Harmon, L. J., J. T. Weir, C. D. Brock, R. E. Glor, and W. Challenger. 2008. GEIGER: Investigating evolutionary radiations. *Bioinformatics* 24:129–131. Oxford University Press.
- Harvey, P. H., and M. D. Pagel. 1991. The comparative method in evolutionary biology. Oxford University Press.
- Hedges, S. B., J. Dudley, and S. Kumar. 2006. TimeTree: A public knowledge-base of divergence times among organisms. *Bioinformatics* 22:2971–2972. Oxford University Press (OUP).
- Hermanson, G., F. V. Iori, S. W. Evers, M. C. Langer, and G. S. Ferreira. 2020. A small podocnemidoid (Pleurodira, Pelomedusoides) from the Late Cretaceous of Brazil, and the innervation and carotid circulation of side-necked turtles. *Pap. Palaeontol.* 6:329–347. Wiley.
- Higham, T. E., L. Schmitz, and K. J. Niklas. 2022. The evolution of mechanical properties of conifer and angiosperm woods. *Integrative and Comparative Biology* 62:668–682. Oxford University Press (OUP).
- Hohenlohe, P. A., and S. J. Arnold. 2008. MIPoD: A hypothesis-testing framework for microevolutionary inference from patterns of divergence. *Am. Nat.* 171:366–385.
- Huang, J.-P., and B. Morgan. 2021. Evolution of adult male horn developmental phenotypes and character displacement in xylotrupes beetles (scarabaeidae). *Ecol. Evol.* 11:5503–5510. Wiley.
- Huang, X., Z. Chen, G. Yang, C. Xia, Q. Luo, X. Gao, and L. Dong. 2022. Assemblages of plasmodium and related parasites in birds with different migration statuses. *Int. J. Mol. Sci.* 23:10277. MDPI AG.
- Huelsenbeck, J. P., R. Nielsen, and J. P. Bollback. 2003. Stochastic mapping of morphological characters. *Syst. Biol.* 52:131–158.
- Huey, R. B., T. Garland Jr, and M. Turelli. 2019. Revisiting a key innovation in evolutionary biology: Felsenstein’s “phylogenies and the comparative method.” *Am. Nat.* 193:755–772. The University of Chicago Press Chicago, IL.
- Huie, J. M., I. Prates, R. C. Bell, and K. de Queiroz. 2021. Convergent patterns of adaptive radiation between island and mainland anolis lizards. *Biol. J. Linn. Soc. Lond.* 134:85–110. Oxford University Press (OUP).
- Hultgren, K. M., S. T. C. Chak, J. Bjelajac, and K. S. Macdonald. 2021. Correlated evolution of larval development, egg size and genome size across two genera of snapping shrimp. *J. Evol. Biol.* 34:1827–1839. Wiley.
- J, L. 2006. Plotrix: A package in the red light district of r. *R-News* 6:8–12.
- Jezovit, J. A., R. Rooke, J. Schneider, and J. D. Levine. 2020. Behavioral and environmental contributions to drosophilid social networks. *Proc. Natl. Acad. Sci. U. S. A.* 117:11573–11583. Proceedings of the National Academy of Sciences.
- King, B., and M. S. Y. Lee. 2015. Ancestral state reconstruction, rate heterogeneity, and the evolution of reptile viviparity. *Systematic Biology* 64:532–544.
- Kirk, E. C., and R. F. Kay. 2004. The evolution of high visual acuity in the anthropeidea. Pp. 539–602 in C. F. Ross and R. F. Kay, eds. *Anthropoid origins: New visions*. Springer US, Boston, MA.
- Lee, M. S. Y., K. L. Sanders, B. King, and A. Palci. 2016. Diversification rates and phenotypic evolution in venomous snakes (Elapidae). *Royal Society Open Science* 3:150277. The Royal Society.
- Lee, M. S. Y., and R. Shine. 1998. Reptilian viviparity and Dollo’s law. *Evolution* 52:1441–1450. Wiley.
- Lewis, P. O. 2001. A likelihood approach to estimating phylogeny from discrete morphological character data. *Syst. Biol.* 50:913–925.

- 1679 Ligges, U., and M. Mächler. 2003. Scatterplot3d - an R package for visualizing multivariate data. *Journal*
1680 *of Statistical Software* 8:1–20.
- 1681 Link, W. A., and R. J. Barker. 2006. Model weights and the foundations of multimodel inference. *Ecology*
1682 87:2626–2635. Wiley.
- 1683 Losos, J. 2009. Lizards in an evolutionary tree: Ecology and adaptive radiation of anoles. University of
1684 California Press.
- 1685 MacPherson, A., S. Louca, A. McLaughlin, J. B. Joy, and M. W. Pennell. 2022. Unifying phylogenetic
1686 birth–death models in epidemiology and macroevolution. *Systematic Biology* 71:172–189. Oxford
1687 University Press (OUP).
- 1688 Maddison, W. P., P. E. Midford, and S. P. Otto. 2007. Estimating a binary character’s effect on speciation
1689 and extinction. *Syst. Biol.* 56:701–710.
- 1690 Maechler, M., C. Dutang, and V. Goulet. 2023. Expm: Matrix exponential, log, ‘etc’.
- 1691 Mahler, D. L., L. J. Revell, R. E. Glor, and J. B. Losos. 2010. Ecological opportunity and the rate of
1692 morphological evolution in the diversification of greater antillean anoles. *Evolution* 64:2731–2745.
- 1693 Marazzi, B., C. Ané, M. F. Simon, A. Delgado-Salinas, M. Luckow, and M. J. Sanderson. 2012. Locating
1694 evolutionary precursors on a phylogenetic tree. *Evolution* 66:3918–3930.
- 1695 Martin, B. S., G. S. Bradburd, L. J. Harmon, and M. G. Weber. 2022. Modeling the evolution of rates of
1696 continuous trait evolution. *Systematic Biology* 72:590–605. Oxford University Press (OUP).
- 1697 Martinez, Q., J. Clavel, J. A. Esselstyn, A. S. Achmadi, C. Grohe, N. Piro, and P.-H. Fabre. 2020.
1698 Convergent evolution of olfactory and thermoregulatory capacities in small amphibious mammals.
1699 *Proc. Natl. Acad. Sci. U. S. A.* 117:8958–8965. Proceedings of the National Academy of Sciences.
- 1700 Martins, B. O., L. Franco-Belussi, M. S. Siqueira, C. E. Fernandes, and D. B. Provete. 2021. The
1701 evolution of red blood cell shape in fishes. *J. Evol. Biol.* 34:537–548. Wiley.
- 1702 McLaughlin, A., V. Montoya, R. L. Miller, G. J. Mordecai, Canadian COVID-19 Genomics Network
1703 (CanCOGen) Consortium, M. Worobey, A. F. Y. Poon, and J. B. Joy. 2022. Genomic epidemiology of
1704 the first two waves of SARS-CoV-2 in Canada. *Elife* 11:e73896. eLife Sciences Publications, Ltd.
- 1705 Medina, I., and N. E. Langmore. 2016. The evolution of host specialisation in avian brood parasites.
1706 *Ecology Letters* 19:1110–1118. Wiley.
- 1707 Microsoft, and S. Weston. 2022. Foreach: Provides foreach looping construct.
- 1708 Mifsud, J. C. O., V. A. Costa, M. E. Petrone, E. M. Marzinelli, E. C. Holmes, and E. Harvey. 2023.
1709 Transcriptome mining extends the host range of the flaviviridae to non-bilaterians. *Virus Evol.*
1710 9:veac124. Oxford University Press (OUP).
- 1711 Mitov, V., K. Bartoszek, and T. Stadler. 2019. Automatic generation of evolutionary hypotheses using
1712 mixed Gaussian phylogenetic models. *Proceedings of the National Academy of Sciences* 116:16921–
1713 16926. Proceedings of the National Academy of Sciences.
- 1714 Molina-Mora, J. A., D. Chinchilla-Montero, R. Garcia-Batan, and F. Garcia. 2021. Genomic context of
1715 the two integrons of ST-111 pseudomonas aeruginosa AG1: A VIM-2-carrying old-acquaintance and
1716 a novel IMP-18-carrying integron. *Infect. Genet. Evol.* 89:104740. Elsevier BV.
- 1717 Morales-Poole, J. R., C. de Vega, K. Tsuji, H. Jacquemyn, R. R. Junker, C. M. Herrera, C. Michiels, B.
1718 Lievens, and S. Álvarez-Pérez. 2022. Sugar concentration, nitrogen availability, and phylogenetic
1719 factors determine the ability of acinetobacter spp. And rosenbergiella spp. To grow in floral nectar.
1720 *Microbial Ecology* 86:377–391. Springer Science; Business Media LLC.
- 1721 Morlon, H., E. Lewitus, F. Condamine, M. Manceau, J. Clavel, and J. Drury. 2016. RPANDA: An R
1722 package for macroevolutionary analyses on phylogenetic trees. *Methods in Ecology and Evolution*
1723 7:589–597.
- 1724 Morlon, H., M. D. Potts, and J. B. Plotkin. 2010. Inferring the dynamics of diversification: A coalescent
1725 approach. *PLoS Biol.* 8.
- 1726 Moura, A., A. Criscuolo, H. Pouseele, M. M. Maury, A. Leclercq, C. Tarr, J. T. Björkman, T. Dallman, A.
1727 Reimer, V. Enouf, E. Larssonneur, H. Carleton, H. Bracq-Dieye, L. S. Katz, L. Jones, M. Touchon, M.
1728 Tourdjman, M. Walker, S. Stroika, T. Cantinelli, V. Chenal-Francisque, Z. Kucerova, E. P. C. Rocha,
1729 C. Nadon, K. Grant, E. M. Nielsen, B. Pot, P. Gerner-Smidt, M. Lecuit, and S. Brisse. 2016. Whole
1730 genome-based population biology and epidemiological surveillance of listeria monocytogenes. *Nat.*
1731 *Microbiol.* 2:16185.
- 1732 Nee, S., R. M. May, and P. H. Harvey. 1994. The reconstructed evolutionary process. *Philos. Trans. R.*
1733 *Soc. Lond. B Biol. Sci.* 344:305–311.

- 1734 Nee, S., A. O. Mooers, and P. H. Harvey. 1992. Tempo and mode of evolution revealed from molecular
1735 phylogenies. *Proceedings of the National Academy of Sciences* 89:8322–8326. *Proceedings of the*
1736 *National Academy of Sciences*.
- 1737 Neuwirth, E. 2022. RColorBrewer: ColorBrewer palettes.
- 1738 Nielsen, R. 2002. Mapping mutations on phylogenies. *Systematic Biology* 51:729–739. Oxford University
1739 Press (OUP).
- 1740 Nunn, C. L. 2011. The comparative approach in evolutionary anthropology and biology. University of
1741 Chicago Press.
- 1742 O'Meara, B. C., C. Ané, M. J. Sanderson, and P. C. Wainwright. 2006. Testing for different rates of
1743 continuous trait evolution using likelihood. *Evolution* 60:922–933.
- 1744 O'Meara, B. C. 2012. Evolutionary inferences from phylogenies: A review of methods. *Annual Review of*
1745 *Ecology, Evolution, and Systematics* 43:267–285. *Annual Reviews*.
- 1746 Osuna-Mascaró, C., A. C. Agneray, L. M. Galland, E. A. Leger, and T. L. Parchman. 2023. Fine-
1747 scale spatial genetic structure in a locally abundant native bunchgrass (*Achnatherum thurberianum*)
1748 including distinct lineages revealed within seed transfer zones. *Evolutionary Applications* 16:979–996.
1749 Wiley.
- 1750 Page, R. D. M. 1993. Parasites, phylogeny and cospeciation. *International Journal for Parasitology*
1751 23:499–506. Elsevier BV.
- 1752 Pagel, M. 1994. Detecting correlated evolution on phylogenies: A general method for the comparative
1753 analysis of discrete characters. *Proc. R. Soc. Lond. B Biol. Sci.* 255:37–45. The Royal Society.
- 1754 Pagel, M. 1999. Inferring the historical patterns of biological evolution. *Nature* 401:877–884.
- 1755 Paradis, E., J. Claude, and K. Strimmer. 2004. APE: Analyses of phylogenetics and evolution in R
1756 language. *Bioinformatics* 20:289–290. academic.oup.com.
- 1757 Paradis, E., and K. Schliep. 2019. Ape 5.0: An environment for modern phylogenetics and evolutionary
1758 analyses in R. *Bioinformatics* 35:526–528. Oxford University Press.
- 1759 Pennell, M. W., J. M. Eastman, G. J. Slater, J. W. Brown, J. C. Uyeda, R. G. FitzJohn, M. E. Alfaro, and L.
1760 J. Harmon. 2014. Geiger v2. 0: An expanded suite of methods for fitting macroevolutionary models
1761 to phylogenetic trees. *Bioinformatics* 30:2216–2218. Oxford University Press.
- 1762 Penny, D., B. J. McComish, M. A. Charleston, and M. D. Hendy. 2001. Mathematical elegance with
1763 biochemical realism: The covarion model of molecular evolution. *Journal of Molecular Evolution*
1764 53:711–723.
- 1765 Pepke, M. L., and D. T. A. Eisenberg. 2022. On the comparative biology of mammalian telomeres:
1766 Telomere length co-evolves with body mass, lifespan and cancer risk. *Mol. Ecol.* 31:6286–6296.
1767 Wiley.
- 1768 Pinheiro, J. C., and D. M. Bates. 2000. Mixed-effects models in s and s-PLUS. Springer, New York.
- 1769 Pinheiro, J., D. Bates, and R Core Team. 2022. Nlme: Linear and nonlinear mixed effects models.
- 1770 Plummer, M., N. Best, K. Cowles, and K. Vines. 2006. CODA: Convergence diagnosis and output
1771 analysis for MCMC. *R News* 6:7–11.
- 1772 Popescu, A.-A., K. T. Huber, and E. Paradis. 2012. Ape 3.0: New tools for distance-based phylogenetics
1773 and evolutionary analysis in R. *Bioinformatics* 28:1536–1537. Oxford University Press (OUP).
- 1774 Poulakakis, N., J. M. Miller, E. L. Jensen, L. B. Beheregaray, M. A. Russello, S. Glaberman, J. Boore,
1775 and A. Caccone. 2020. Colonization history of Galapagos giant tortoises: Insights from mitogenomes
1776 support the progression rule. *Journal of Zoological Systematics and Evolutionary Research* 58:1262–
1777 1275. Hindawi Limited.
- 1778 Pozzi, L., M. Voskamp, and P. M. Kappeler. 2022. The effects of body size, activity, and phylogeny on
1779 primate sleeping ecology. *Am. J. Biol. Anthropol.* 179:598–608. Wiley.
- 1780 Pybus, O. G., and P. H. Harvey. 2000. Testing macro-evolutionary models using incomplete molecular
1781 phylogenies. *Proc. Biol. Sci.* 267:2267–2272.
- 1782 Qiu, W., and H. Joe. 2020. clusterGeneration: Random cluster generation (with specified degree of
1783 separation).
- 1784 Quach, Q. N., R. G. Reynolds, and L. J. Revell. 2019. Historical allopatry and secondary contact or
1785 primary intergradation in the puerto rican crested anole, *Anolis cristatellus*, on Vieques Island in the
1786 Caribbean. *Biol. J. Linn. Soc. Lond.* Oxford University Press (OUP).
- 1787 R Core Team. 2023. R: A language and environment for statistical computing. R Foundation for Statistical
1788 Computing, Vienna, Austria.

- 1789 Rabosky, D. L. 2014. Automatic detection of key innovations, rate shifts, and diversity-dependence on
1790 phylogenetic trees. *PLoS One* 9:e89543. Public Library of Science.
- 1791 Revell, L. J. 2021. A variable-rate quantitative trait evolution model using penalized-likelihood. *PeerJ*
1792 9:e11997. PeerJ.
- 1793 Revell, L. J. 2014a. Ancestral character estimation under the threshold model from quantitative genetics.
1794 *Evolution* 68:743–759.
- 1795 Revell, L. J. 2018. Comparing the rates of speciation and extinction between phylogenetic trees. *Ecol.*
1796 *Evol.* 8:5303–5312.
- 1797 Revell, L. J. 2014b. Graphical methods for visualizing comparative data on phylogenies. Pp. 77–103 *in*
1798 *Modern phylogenetic comparative methods and their application in evolutionary biology*. Springer
1799 Berlin Heidelberg.
- 1800 Revell, L. J. 2012. phytools: An R package for phylogenetic comparative biology (and other things).
1801 *Methods Ecol. Evol.* 3:217–223. Wiley Online Library.
- 1802 Revell, L. J. 2009. Size-correction and principal components for interspecific comparative studies.
1803 *Evolution* 63:3258–3268. Wiley Online Library.
- 1804 Revell, L. J. 2013. Two new graphical methods for mapping trait evolution on phylogenies. *Methods Ecol.*
1805 *Evol.* 4:754–759. Wiley.
- 1806 Revell, L. J., and D. C. Collar. 2009. Phylogenetic analysis of the evolutionary correlation using likelihood.
1807 *Evolution* 63:1090–1100.
- 1808 Revell, L. J., L. E. Gonzalez-Valenzuela, A. Alfonso, L. A. Castellanos-Garcia, C. E. Guarnizo, and A. J.
1809 Crawford. 2018. Comparing evolutionary rates between trees, clades and traits. *Methods Ecol. Evol.*
1810 9:994–1005. Wiley Online Library.
- 1811 Revell, L. J., and L. J. Harmon. 2022. *Phylogenetic comparative methods in R*. Princeton University
1812 Press, Princeton, NJ.
- 1813 Revell, L. J., L. J. Harmon, and D. C. Collar. 2008. Phylogenetic signal, evolutionary process, and rate.
1814 *Syst. Biol.* 57:591–601.
- 1815 Revell, L. J., and A. S. Harrison. 2008. PCCA: A program for phylogenetic canonical correlation analysis.
1816 *Bioinformatics* 24:1018–1020. Oxford University Press (OUP).
- 1817 Revell, L. J., M. A. Johnson, J. A. Schulte 2nd, J. J. Kolbe, and J. B. Losos. 2007. A phylogenetic test for
1818 adaptive convergence in rock-dwelling lizards. *Evolution* 61:2898–2912. Wiley.
- 1819 Revell, L. J., D. L. Mahler, P. R. Peres-Neto, and B. D. Redelings. 2012. A new phylogenetic method for
1820 identifying exceptional phenotypic diversification. *Evolution* 66:135–146.
- 1821 Revell, L. J., D. L. Mahler, R. G. Reynolds, and G. J. Slater. 2015. Placing cryptic, recently extinct, or
1822 hypothesized taxa into an ultrametric phylogeny using continuous character data: A case study with
1823 the lizard *Anolis roosevelti*. *Evolution* 69:1027–1035. Wiley.
- 1824 Revell, L. J., K. S. Toyama, and D. L. Mahler. 2022. A simple hierarchical model for heterogeneity in the
1825 evolutionary correlation on a phylogenetic tree. *PeerJ* 10:e13910. PeerJ.
- 1826 Roy, V. 2020. Convergence diagnostics for markov chain monte carlo. *Annual Review of Statistics and*
1827 *Its Application* 7:387–412. Annual Reviews.
- 1828 RStudio Team. 2020. *RStudio: Integrated development environment for r*. RStudio, PBC., Boston, MA.
- 1829 Sánchez-Busó, L., D. Golparian, J. Corander, Y. H. Grad, M. Ohnishi, R. Flemming, J. Parkhill, S. D.
1830 Bentley, M. Unemo, and S. R. Harris. 2019. The impact of antimicrobials on gonococcal evolution.
1831 *Nat. Microbiol.* 4:1941–1950. Springer Science; Business Media LLC.
- 1832 Sander, P. M., E. M. Griebeler, N. Klein, J. V. Juarbe, T. Wintrich, L. J. Revell, and L. Schmitz. 2021.
1833 Early giant reveals faster evolution of large body size in ichthyosaurs than in cetaceans. *Science*
1834 374:eabf5787. American Association for the Advancement of Science (AAAS).
- 1835 Schliep, K. P. 2011. Phangorn: Phylogenetic analysis in R. *Bioinformatics* 27:592–593.
- 1836 Schluter, D., T. Price, A. Ø. Mooers, and D. Ludwig. 1997. Likelihood of ancestor states in adaptive
1837 radiation. *Evolution* 51:1699–1711. Wiley.
- 1838 Sidlauskas, B. 2008. Continuous and arrested morphological diversification in sister clades of characiform
1839 fishes: A phylomorphospace approach. *Evolution* 62:3135–3156. Wiley.
- 1840 Stadler, T. 2013. How can we improve accuracy of macroevolutionary rate estimates? *Syst. Biol.*
1841 62:321–329. Oxford University Press (OUP).
- 1842 Stadler, T. 2011. Inferring speciation and extinction processes from extant species data. *Proc. Natl. Acad.*
1843 *Sci. U. S. A.* 108:16145–16146. National Acad Sciences.

- 1844 Stadler, T. 2019. TreeSim: Simulating phylogenetic trees.
- 1845 Stull, G. W., P. S. Soltis, D. E. Soltis, M. A. Gitzendanner, and S. A. Smith. 2020. Nuclear phylogenomic
- 1846 analyses of asterids conflict with plastome trees and support novel relationships among major lineages.
- 1847 American Journal of Botany 107:790–805. Wiley.
- 1848 Uetz, P., P. Freed, R. Aguilar, F. Reyes, and J. Hošek. 2023. The Reptile Database.
- 1849 Uyeda, J. C., and L. J. Harmon. 2014. A novel Bayesian method for inferring and interpreting the
- 1850 dynamics of adaptive landscapes from phylogenetic comparative data. Syst. Biol. 63:902–918.
- 1851 Valles-Colomer, M., G. Falony, Y. Darzi, E. F. Tigchelaar, J. Wang, R. Y. Tito, C. Schiweck, A. Kurilshikov,
- 1852 M. Joossens, C. Wijmenga, S. Claes, L. Van Oudenhove, A. Zhernakova, S. Vieira-Silva, and J. Raes.
- 1853 2019. The neuroactive potential of the human gut microbiota in quality of life and depression. Nat.
- 1854 Microbiol. 4:623–632. Springer Science; Business Media LLC.
- 1855 Van Borm, S., G. Boseret, S. Dellicour, M. Steensels, V. Roupie, F. Vandenbussche, E. Mathijs, A.
- 1856 Vilain, M. Driesen, M. Dispas, A. W. Delcloo, P. Lemey, I. Mertens, M. Gilbert, B. Lambrecht, and
- 1857 T. van den Berg. 2023. Combined phylogeographic analyses and epidemiologic contact tracing to
- 1858 characterize atypically pathogenic avian influenza (H3N1) epidemic, belgium, 2019. Emerg. Infect.
- 1859 Dis. 29:351–359. Centers for Disease Control; Prevention (CDC).
- 1860 van der Walt, S., and N. Smith. 2015. A better default colormap for Matplotlib. SciPy 2015.
- 1861 Venables, W. N., and B. D. Ripley. 2002. Modern applied statistics with S. Fourth. Springer, New York.
- 1862 Venditti, C., A. Meade, and M. Pagel. 2011. Multiple routes to mammalian diversity. Nature 479:393–396.
- 1863 Springer Science; Business Media LLC.
- 1864 Xie, Y. 2023. Bookdown: Authoring books and technical documents with r markdown.
- 1865 Xie, Y. 2016. Bookdown: Authoring books and technical documents with R markdown. Chapman;
- 1866 Hall/CRC, Boca Raton, Florida.
- 1867 Xie, Y., J. J. Allaire, and G. Grolemond. 2018. R markdown: The definitive guide. Chapman; Hall/CRC,
- 1868 Boca Raton, Florida.
- 1869 Xie, Y., C. Dervieux, and E. Riederer. 2020. R markdown cookbook. Chapman; Hall/CRC, Boca Raton,
- 1870 Florida.
- 1871 Yang, Z. 2014. Molecular Evolution: A Statistical Approach. Oxford University Press, London, England.